Coordinating Signaling Pathways Between Cell Types to Control Anterior Morphogenesis *in C. elegans*

Victoria Richard

A thesis
in
The Department
of
Biology

Presented in Partial Fulfilment of the Requirements
for the Degree of Masters in Science (Biology) at
Concordia University
Montreal, Quebec, Canada

August 2021

CONCORDIA UNIVERSITY

School of Graduate Studies

This is to certify that the thesis prepared

By: Victoria Richard

Entitled: Coordinating signaling pathways between cell types to control anterior morphogenesis

and submitted in partial fulfillment of the requirements for the degree of

Master of Science (Biology)

complies with the regulations of the University and meets the accepted standards with respect to originality and quality.

Signed by the Examining Committee:

_____ Chair

Dr. Christopher Brett

_____ External Examiner

Dr. Malcolm Whiteway

_____ Examiner

Dr. William Zerges

_____ Thesis Supervisor

Dr. Alisa Piekny

Approved by _____

Dr. Robert Weladji, Graduate Program Director

August 25th 2021 _____

Dr. Pascale Sicotte, Dean of Faculty

ABSTRACT

Coordinating signaling pathways between cell types to control anterior morphogenesis in C. elegans

Victoria Richard

Morphogenesis is crucial for the development of tissues which must be coordinated to give rise to complex structures in the context of an organism. Mechanisms at the single cell, tissue and multi-tissue levels contribute to the complexities in studying morphogenesis. In *C. elegans*, prior studies uncovered mechanisms regulating epidermal and pharyngeal morphogenesis, but how these and other tissues are coordinated to give rise to the anterior lumen remained a black box. We characterized anterior morphogenesis to determine how the epidermal, pharyngeal and neuroblast (neuronal precursor) cells move and are positioned relative to one another, and to identify signaling events that regulate their coordination. We found that the first visible marker of the future anterior lumen are projections from the anterior-most pharyngeal cells (arcade cells) which form a stable rosette and express the polarity protein PAR-6. These projections are surrounded by subsets of polarized neuroblasts with PAR-6-enriched projections that organize into patterns forming two pentagons and a semi-circle. The anterior epidermal cells migrate toward the projections and ultimately join with the pharyngeal cells for their successful epithelialization. We found that the ventral epidermal cells migrate using F-actin-rich projections which come close to, but do not cross the semi-circle of foci suggesting that the cells corresponding to these foci provide guidance cues. Blocking neuroblast cell division and disrupting the patterns of polarized neuroblasts caused a decrease in the number of epidermal F-actin projections and delayed their migration. We propose that signals associated with the neuronal and/or glial cells control anterior epidermal cell migration. To identify these signals, we performed RNAi to several guidance cues and their receptors, and found that slit (*slt-1*) and sax/robo (*sax-3*) are required for neuroblast positioning and epidermal cell migration. This work provides new insights on the mechanisms underlying the multi-tissue cooperation required for successful anterior morphogenesis of *C. elegans* embryos.

Acknowledgements

I would like to thank Dr. Alisa Piekny for being a wonderful supervisor and mentor over the past three years. You have taught me many things inside and outside of the lab and I could not have been happier working under a strong woman such as yourself.

I would like to thank my committee members, Dr. William Zerges, Dr. Christopher Brett and Dr. Malcolm Whiteway for their time and support during this project.

Additionally, I would like to thank Dr. Chris Law for all his help at *The Centre for Microscopy and Imaging*. May you never have to locate embryos on a microscope ever again.

Lastly, I would like to thank all the Piekny lab members. To Karina & Steph, thank you for welcoming me onto your team so graciously. Imge, thank you for introducing me to the worms and for all the moral support. To Khash, thank you for all your efforts during your 490. To Matthew, thank you for all your help with the worm stuff and all the friendship! And finally, to Joe, Kevin, Nhat, Mathieu, Adryanne, Su pin & Noha thank you for making the lab a pleasant place to work full of friendly faces.

Dedications

This thesis is dedicated to my family and friends. Thank you for being so supportive of the worms and I despite having no clue what I have been talking about the past three years. To my mom, who still sometimes thinks I am studying chemistry, thank you for pushing me and supporting me to achieve my goals. To my sisters, thank you for making "study parties" a thing. I honestly think no one makes being a nerd look better (or easier) than you ladies. And to my dear friend Joe, thank you for being my Master's twin and doing this journey with me. I can't imagine what it would have been like without you and I will cherish our memories forever!

Contribution of authors

Figure 7. Karina Mastronardi & Stephanie Grimbert contributed equally to this figure.

Figure 8. Karina Mastronardi & Stephanie Grimbert contributed equally to A, B and C of this figure. Strain generated and imaged for D completed by myself, Karina Mastronardi & Stephanie Grimbert produced the figure.

Figure 9. Imaging completed by myself, Karina Mastronardi & Stephanie Grimbert produced the figure.

Figure 10. Karina Mastronardi & Stephanie Grimbert contributed equally to A and B of this figure. Imaging for C and E completed by myself, while Karina Mastronardi & Stephanie Grimbert made the figure.

Figure 11. Karina Mastronardi & Stephanie Grimbert contributed equally to A, B and C of this figure.

Figure 12. Imaging completed by myself, while Karina Mastronardi & Stephanie Grimbert contributed the data analysis.

Figure 13. Figure contributed entirely by myself.

All authors reviewed the final manuscript and approved of the contents.

Table of Contents

List of Figures

CHAPTER 1
Introduction

1.1 Introduction

How multiple tissue types come together during their morphogenesis to form complex structures during development remains poorly understood. This is mainly due to the challenges of studying how cells from different tissues are coordinated *in vivo*. Model organisms have proven invaluable for improving our understanding of how chemical and mechanical cues between cells within a single tissue can govern specific morphogenetic events, but very few studies have been done at the multi-tissue level. Morphogenesis requires the tight coordination of cell shape changes and migration, where cells need to be in specific positions and/or form distinct patterns for development to occur properly. *C. elegans* are a powerful model for studying morphogenesis as they are amenable to microscopy techniques that permit the visualization of cell shape changes and migration in the context of their native environment. The lineage of each of the nine-hundred and fifty-nine somatic cells in the adult hermaphrodite has been mapped, making C. elegans amenable to studies of more complex developmental processes that require multiple cell types/tissues.

Some of the first examples of tissue-tissue communication were revealed in *C. elegans*. For example, during epidermal morphogenesis, chemical signaling between the neuroblasts and epidermal cells drives ventral enclosure, when the ventral epidermal cells cover the belly of the embryo in a layer of epidermis (e.g. Ghenea et al., 2005; Ikegami et al., 2012). At a later stage of epidermal morphogenesis, contraction of the newly formed muscle cells drives epidermal cell (also called hypodermis) shape changes for elongation via mechanotransduction (Williams & Waterston, 1994; Zhang et al., 2011). The muscle sarcomeres are connected to epidermal cell F-

actin through integrins and focal adhesions, so that force generated by contraction of the muscle fibres is transduced to the epidermal F-actin where it mediates cell elongation (Gettner et al., 1995; Zhang et al., 2011; Lecroisey et al., 2007). During vulval development, which occurs at the L4 stage, chemical signals from the anchor cell to the nearby vulval precursor cells (derived from the hypodermis) causes them to differentiate into the vulva (Sternberg, 2005). For example, a long-range spatial gradient of epidermal growth factor (EGF) and a cell-to-cell signal via the Notch-like receptor LIN-12 are both involved in inducing vulval cell fate (Sternberg, 1988; Sternberg & Horvitz, 1986). Subsequent studies found that other pathways also contribute to vulval cell fate, including WNT signalling (Sternberg, 2005). Due to the complex network of spatiotemporal signaling, *C. elegans* vulval development has become a model for animal organogenesis. However, complex structures that require the coordination of more than two tissue types remain poorly understood. In particular, the processes that coordinate development of the epidermal, neuronal and pharyngeal tissues for anterior morphogenesis would provide a model for how these events occur in more complex organisms.

1.2 *C. elegans* morphogenesis

In the 16 hours required for *C. elegans* to complete embryogenesis, multiple morphogenetic events occur for the zygote to develop into the first larval stage (Figure 1). Gastrulation occurs at the 24-cell stage when the E (endoderm) daughter cells ingress into the interior of the embryo (Skiba & Schierenberg, 1992). Their inward movement creates a depression on the ventral side of the embryo called the ventral cleft, which is closed by anteriorly migrating neuroblast cells (Sulston et al., 1983). This is followed by the onset of epidermal morphogenesis, when dorsal intercalation occurs after the epidermal cells are born on the dorsal surface of the

embryo (Chisholm & Hardin, 2005). During this time, two rows of dorsal epidermal cells change shape and interdigitate with one another to form a single row of cells along the dorsal midline (Williams-Masson et al., 1998). Subsequently, ventral epidermal cells migrate towards the ventral midline to encase the embryo in a layer of epidermis in a process called ventral enclosure (Williams-Masson et al., 1997). The leading pair of ventral epidermal cells extend actin-based protrusions as they migrate over the neuroblasts toward their contralateral partners (Raich et al., 1999). This is followed by the formation of a pocket formed by the posterior ventral epidermal cells which closes via a purse-string like mechanism in a supracellular (or tissue level) manner via coordinated actomyosin contractility across multiple cells (Fotopoulos et al., 2013; Wernike et al., 2016; Williams-Masson et al., 1997). During ventral enclosure, the anterior-most epidermal cells begin to migrate toward the anterior where they must ultimately coordinate with the developing pharynx and underlying neuroblasts. The pharyngeal cells polarize and form an epithelialized lumen that connects the buccal cavity (mouth) with the intestine. During this process, the pharynx attaches to the anterior and forms a sensory depression at the location of the future mouth, which also aligns with groups of neurons that migrate anteriorly to form the head sensilla. As the embryo progresses through mid-late embryogenesis, the epidermis undergoes elongation concomitant with when the muscle cells differentiate and begin to contract. Lateral hypodermal cell shape changes are the driving force that lengthens the embryo along the anterior-posterior axis to form the vermiform shape of the worm (Priess and Hirsh, 1986; Wissmann et al., 1997; Piekny et al., 2000). The coordination of migration and shape changes among cells from different tissues presumably requires tightly regulated chemical and/or mechanical signaling, although these are still not well-understood for most stages of embryogenesis.

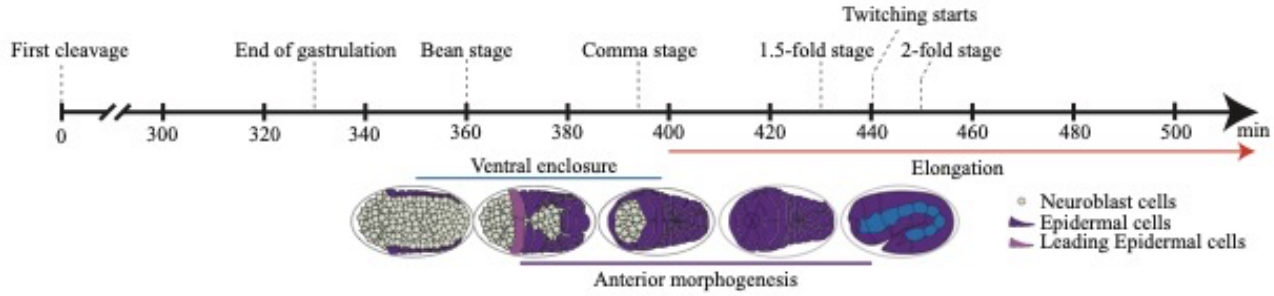

Figure 1. Timing of morphogenetic events during *C. elegans* embryogenesis. The timeline (in minutes) shows the key morphogenetic events that occur during *C. elegans* embryogenesis. Anterior morphogenesis begins when the leading pair of migrating epidermal cells meet at the ventral midline (t = ~380) and continues throughout ventral enclosure and part of elongation (~440 minutes/twitching stage). Adapted from Grimbert et al., 2021.

1.2.1 Cell polarity and patterning

Cellular processes, including migration and shape changes, rely on polarity. Polarity is defined by spatial differences in the structure and localization of components within a cell. Polarity is initiated and established by intrinsic or extrinsic cues that cause distinct domains to form in the cell which are reinforced by trafficking (Drubin & Nelson, 1996). Small GTPases play an important role in the reorganization of the actin-myosin cytoskeleton required for inducing and maintaining polarity. For example, the localized activation of RhoA directs actin polymerization and non-muscle myosin activation within a specific region of the cell that can generate changes in cell shape (Ouellette et al., 2016). Localized Cdc42 activation via directed vesicle trafficking reinforces these changes (Ouellette et al., 2016).

Proteins that have conserved roles in regulating cell polarity in metazoans include the PAR proteins, which were initially discovered in screens for mutations that disrupt asymmetric cell division in *C. elegans.* In *C. elegans*, the PAR (partitioning-defective) proteins are required to establish and maintain anterior-posterior polarity in the early embryo for asymmetric division to give rise to cells of different fates, and to form apicobasal polarity in the lumen-facing cells in the pharynx and gut (Rasmussen et al., 2012). The distribution of PAR proteins and how they define areas of specialization is a hallmark of cell polarity in metazoans (Hoege & Hyman, 2013). In the *C. elegans* zygote, PAR proteins are partitioned into two distinct cortical domains that define the anterior and posterior regions of the cortex (Figure 2; Hoege & Hyman, 2013). The anterior complex contains PAR-3, PAR-6, and atypical protein kinase C-like (PKC-3) which can bind to active CDC-42, whereas the posterior complex contains PAR-1, PAR-2 and LGL-1 (Beatty et al., 2010; Watts et al., 1996). Prior to fertilization, the entire cortex is contractile and enriched in active RHO-1, which then dampens at the posterior cortex after sperm entry (Motegi & Sugimoto, 2006).

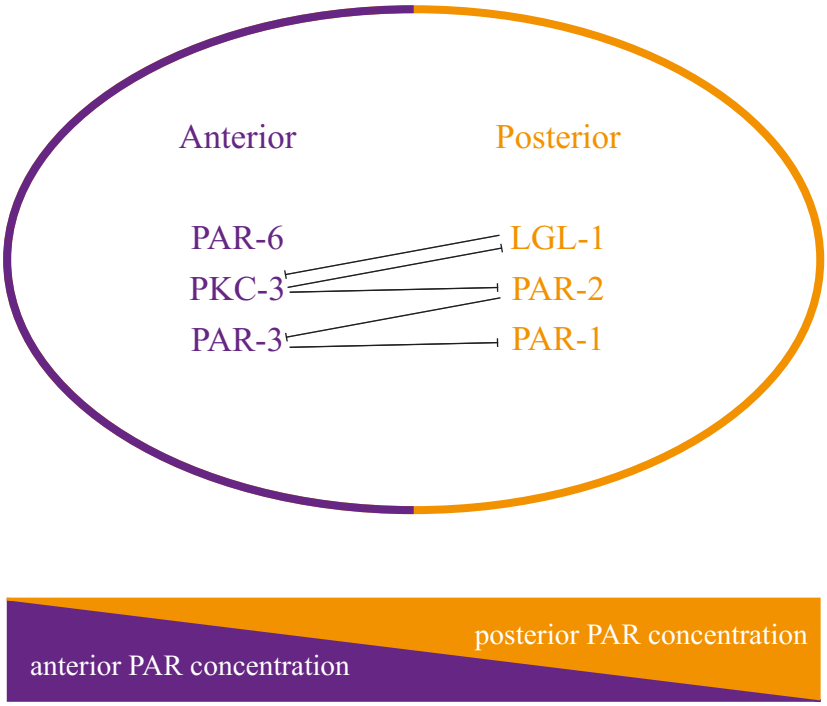

Figure 2. Polarity protein complexes in the early *C. elegans* embryo. A schematic shows the localization of anterior (purple) and posterior (orange) PAR protein complexes in polarized embryos (above) and enrichment (concentrations) in the anterior-posterior axis (below). The anterior complex (PAR-3, PAR-6 and PKC-3) is most concentrated at the anterior, while the posterior-defining complex (PAR-2, PAR-2, LGL-1) is most concentrated at the posterior, however there is no overlap between the localized complexes. Mutual inhibition (shown by arrows) via kinase components of each complex causes the removal of the other components from the cortex. Adapted from Hoege & Hyman., 2013.

This generates cortical flows that help to localize proteins along the anterior-posterior axis (Munro et al., 2004). Subsequently, active CDC-42 binds to PAR-6 in the anterior and helps to maintain polarity. A boundary is formed at the interface of the anterior and posterior PAR domains through mutual-inhibition, where the anterior PAR complex phosphorylates and inhibits the localization of the posterior PAR complex and vice versa (Figure 2; Hoege & Hyman, 2013). Anterior-posterior asymmetry is required to localize cell fate determinants and position the spindle to ensure that the daughter cells acquire the right fate (Hoege & Hyman, 2013).

Epithelial cells also rely on PAR proteins to define apicobasal polarity in metazoans. In particular, a complex containing Par3, Par6 and aPKC localizes to the apical cortex via active Cdc42, while the Scribble complex with Scribble, Lgl and Dlg1 defines the basolateral region (Bilder et al., 2003; Rodriguez-Boulan & Macara, 2014) These mutually exclusive domains are defined by adherens and tight junctions, which adhere cells to their neighbours. Adherens junctions connect intracellular actomyosin filaments at a supracellular level to transmit force across the tissue, while tight junctions control permeability between cells. Whereas vertebrate cells contain distinct adhesion and tight junctions, *C. elegans* epithelial cells have a single junction with a mix of both components (Figure 3). The core adherens junction components are conserved and include HMR-1/E-cadherin, HMP-2/ β-catenin, and HMP-1/ α-catenin, also referred to as the cadherin-catenin complex (CCC). These components are required for proper epidermal morphogenesis (Costa et al., 1998). Claudins (VAB-9, CLC-1) are also part of the *C. elegans* junction, whereas they are restricted to tight junctions in mammalian cells. *C. elegans* also has another complex within their junction referred to as the DAC, which consists of DLG-1 (Discs-large) and AJM-1 and localizes more basal compared to the CCC (Figure 3; reviewed by Labouesse, 2006).

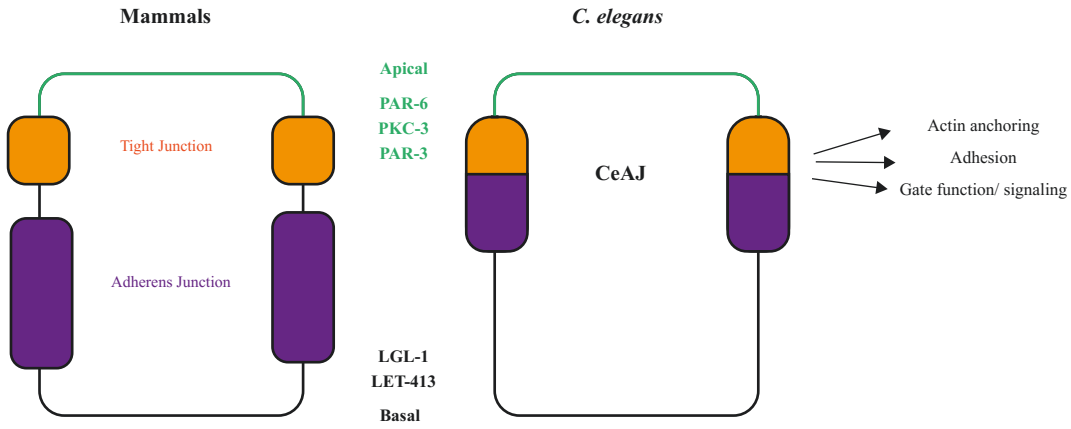

Figure 3. Epithelial cell junctions in *C. elegans* and mammals. Schematics compare cell junctions in *C. elegans* and mammalian epithelial cells. While mammalian cells (left) have distinct tight (orange) and adherens junctions (purple), *C. elegans* cells (right) have one junction that contains conserved components of each. In mammalian and *C. elegans* cells, the junctions define the apical (green; PAR-6, PKC-3, PAR-3) and basolateral domains (black; LGL-1/Lgl, LET-413/Scribble) of the cell. Conserved components of adherens junctions include the cadherin-catenin complex (CCC; E-cadherin/HMR-1, alpha-/HMP-1 and beta-catenin/HMP-2). *C. elegans* also have DLG-1 and AJM-1 (DAC), which is not conserved in mammals. *C. elegans* junctions also contain tight junction components including the claudins (VAB-9 and CLC-1). Adapted from Armanti & Nance., 2013.

Cellular patterns arise from groups of cells that respond to positional cues. A well-known example of patterns formed by polarized cells are rosettes, which help drive morphogenesis (Blankenship et al., 2006). Rosettes are formed from five or more cells that interface at a central point along either the planar or apical axis (Figure 4). Planar rosettes require planar cell polarity and help coordinate the re-positioning of cells from one axis to another. Planar rosettes are commonly formed during convergent extension, which is the narrowing of tissues along one axis while elongating them along the perpendicular axis via cell intercalation (Shah et al., 2017). Apical rosettes require cells to undergo apical constriction, and these stable patterns give rise to lumens (Harding et al., 2014). Actomyosin contractility drives the shape changes required for either type of rosette. In addition, while transient, planar rosettes are coupled with the disassembly and reassembly of junctions as cells form new neighbours, the apical rosettes formed from teardrop-shaped cells are coupled supracellularly through adhesion junctions (Martin & Goldstein, 2014). Rosettes are an example of how polarity drives changes in cell position for tissue morphogenesis and lumen formation.

In this work, I describe interesting patterns that form at the anterior of embryo during mid-embryogenesis formed by cells expressing fluorescently tagged PAR-6, required for apicobasal polarity. One of these patterns includes a stable apical rosette which corresponds to the anterior lumen, while other patterns have not been previously described. Although not fully understood, we believe that the polarized cells contributing to these patterns provide and/or respond to cues required for epidermal cell migration during anterior morphogenesis.

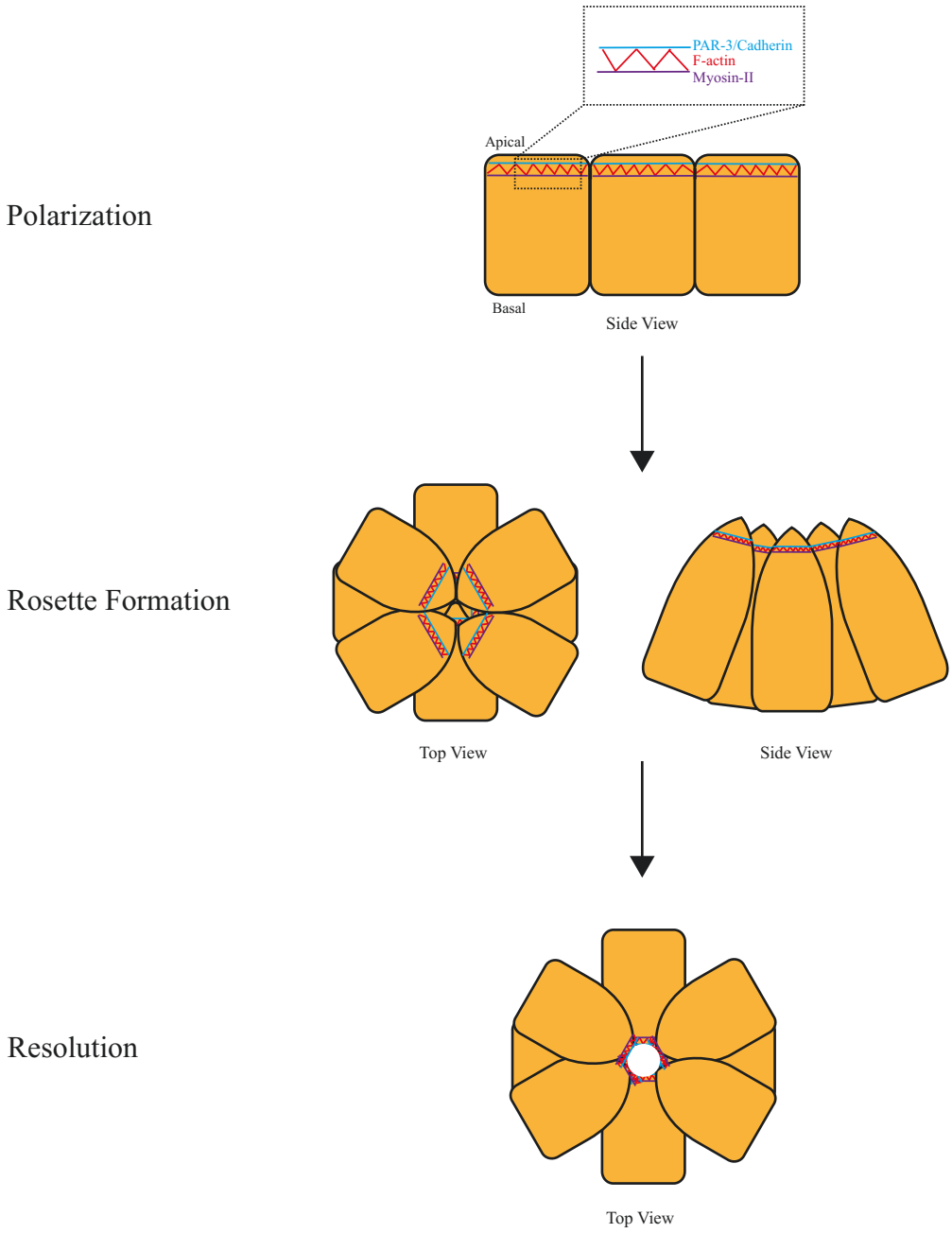

Figure 4. Mechanisms of apically forming rosettes. Schematics show a stable rosette formed by cells that have undergone apical constriction. Proteins such as F-actin, myosin-II, PAR-3 and cadherin are localized to (sub)apical domains. The centre of the rosette often forms a central lumen. This figure was adapted from Harding *et al.*, 2014.

1.2.3. Cell migration

Cell polarity is also required to govern cell migration. Generally, cell migration occurs in response to a cue by polarizing and forming protrusions in the direction of migration, followed by contraction in the rear of the cell to generate propulsion and move the cell body forward (Ridley et al., 2003; Rørth, 2009). As the cell moves forward, focal adhesions form in the front of the cell, while those in the rear are disassembled. The lamellipodia or filopodia protrusions formed at the front of migrating cells are actin-based structures that probe the substrate (Figure 5; Ridley et al., 2003). The formation of these structures require the rapid turnover of F-actin, which can be both branched and unbranched, and are under the control of Rac and Cdc42, along with their effectors (Nobes & Hall, 1995). Active Rac and Cdc42 bind to and activate WASp (Wiskott-Aldrich syndrome protein) and WAVE/SCAR (WASp family verprolin homology proteins/suppressor of cAMP receptor) complexes, which then activate Arp2/3 to template the growth of branched F-actin (Goley & Welch, 2006). In the rear, stress fibres are formed from unbranched F-actin bundles via active RhoA, which binds to formin to nucleate profilin-based F-actin, and active RhoA also binds to Rho kinase to generate myosin contractility (Clainche & Carlier, 2008). In this manner, Rac is considered the key regulator of steering, while RhoA generates the force required for movement.

When cells move as a collective, they can maintain some or all aspects of single-celled migration. Collective cell migration coordinates cells so that a tissue remains intact during remodeling (Rørth, 2009). Epithelial tissue morphogenesis in many organisms is an example of collective migration. Epithelial cells are interconnected as a sheet through junctions, which provides continuity among the cells so they can move forward as a sheet. The cells at the leading edge exhibit increased protrusive activity and are known as leader or pioneer cells (Vitorino &

Meyer, 2008). The protrusive free edge versus regions involved in cell-cell contact is induced by their position within the sheet, although the mechanism is not known (Rørth, 2009). When an epithelial sheet encounters a hole or gap, such as the dorsal pocket in Drosophila or the ventral pocket in *C. elegans*, the leading cells can form an actin-rich ring around the gap that contracts to close via a purse-string mechanism (Rodriguez-Diaz et al., 2008; Wernike et al., 2016; Williams-Masson et al., 1997).

During *C. elegans* ventral enclosure, the ventral epidermal cells migrate collectively to enclose the ventral surface of the embryo in a layer of epidermis (Chisholm & Hardin, 2005). As described earlier, ventral enclosure requires the migration of two pairs of leading cells followed by the closure of a ventral pocket formed by the coordinated supracellular constriction of the posterior-positioned ventral epidermal cells (Fotopoulos et al., 2013; Williams-Masson et al., 1997). While the leading cells migrate via mechanisms similar to single cells, the pocket cells migrate in a collective manner, followed by purse-string constriction (Williams-Masson et al., 1997). *C. elegans* homologues of regulators of short-branched F-actin including Arp2/3, WASp (WSP-1), WASp family members (*e.g.* WVE-1) and WAVE/SCAR (GEX-1, GEX-2, GEX-3, ABI-1) are all required for ventral enclosure. For example, embryos with mutations in *gex-2* or *gex-3* have defects in leading ventral epidermal cell migration causing failed ventral enclosure and extrusion of the internal contents (Patel et al., 2008). The leading ventral epidermal cells in *gex-2* or *gex-3* mutant embryos have disorganized F-actin and fail to extend projections (Patel et al., 2008). Conversely, mutations in adhesion complex components (*e.g. hmr-1*, *hmp-1* and *hmp-2*) or those in the RhoA pathway including the RhoGEF/*ect-2*, and the Rho kinase/*let-502* cause defects in ventral pocket closure (Costa et al., 1998; Fotopoulos et al., 2013; Wernike et al., 2016).

1.3 Signaling pathways implicated in tissue morphogenesis

Chemical signaling pathways control several morphogenetic processes including ventral enclosure and neuronal axon guidance, but we still do not have a clear picture of their tissue-specific requirements for these processes, nor their role in anterior morphogenesis. These pathways include well-known ligands such as Slit, Netrin, Ephrin and Semaphorin, and their receptors which have been studied extensively in multiple organisms and contexts.

1.3.1 Signaling during ventral enclosure

The UNC-6/netrin, SLT-1/Slit, VAB-2/Ephrin and MAB-20/Semphorin axonal guidance cues and their receptors, UNC-40/DCC, SAX-3/Robo, VAB-1/Eph, and PLX-2/Plexin, respectively, have all been shown to regulate migration of the ventral epidermal cells. Null mutations in either *vab-1* or *efn-1* give rise to embryos with defective cell movements and severe morphogenesis phenotypes (Chin-Sang et al., 1999). However, the phenotypes are not completely penetrant suggesting genetic redundancy among different signaling pathways. They function upstream of the complexes that control F-actin for epidermal cell migration either directly or indirectly, and is not clear what tissue they are required in (Figure 5; Bernadskaya et al., 2012; Chin-Sang et al., 1999; Ikegami et al., 2012). For example, the ligands could be expressed in the neuroblasts and/or epidermal cells and signal via receptors in the ventral epidermal cells to control their migration via the pathways regulating F-actin, while other receptors are expressed in the neuroblasts and signaling controls their position, which in turn affects epidermal cell position in a mechanical fashion. Several models posit that proper positioning of the developing neuroblasts passively or directly controls migration of the epidermal cells. In either case, epidermal cell migration defects would be caused non-autonomously by improperly positioned neuroblasts. For

example, the VAB-2/EFN-1 ligand is expressed in neuroblasts while its receptor, VAB-1 is expressed in a different subset of neuroblasts. Mutations in both *vab-1* and *vab-2* cause disorganized neuroblasts and epidermal morphogenesis phenotypes during ventral enclosure (Chin-Sang et al., 1999). Work from our lab further reinforced this model, where we found that ANI-1 is expressed in the neuroblasts and not epidermal cells during ventral enclosure and is required for their division (Fotopoulos et al., 2013). Depletion of *ani-1* caused ventral enclosure defects, largely due to disorganized closure of the ventral pocket cells (Wernike et al., 2016).

A study by Ikegami *et al* (2012) showed that the semaphorin pathway functions alongside the ephrin pathway. Neuroblasts expressing PLX-2 and VAB-1 align themselves with bilateral symmetry to form a bridge. This bridge directs epidermal cell migration toward the ventral midline (Ikegami et al., 2012). The enhanced ventral enclosure phenotypes in *vab-1* and *plx-2* or *mab-20* double mutants suggests redundancy between the two pathways, and implicates semaphorin signaling in proper neuroblast positioning and ventral enclosure, similar to the ephrin pathway (Ikegami et al., 2012).

The Slit/Robo pathway also controls ventral enclosure. Embryos mutant for *sax-3* display ventral enclosure defects comparable to embryos mutant for ephrin pathway components (Ghenea et al., 2005). Embryos that are double mutant for *sax-3* and *vab-1* have a completely penetrant embryonic lethal phenotype. Since SAX-3 and VAB-1 colocalize within neuroblasts, one model is that SAX-3 and VAB-1 function together to coordinate neuroblast positioning, with SAX-3 directly signaling to the epidermal cells to control their migration (Ghenea et al., 2005).

Some of the same pathways governing neuroblast positioning and ventral epidermal cell migration are also known to regulate axon guidance. In general, the Robo family of receptors and Slit ligands are evolutionarily conserved and have been studied for their function in mediating

axonal guidance in multiple organisms (Brose et al., 1999). In *C. elegans*, SAX-3 has been implicated in various axonal guidance events including nerve ring positioning, while the semaphorin signaling component PLX-2 regulates migration of the sublateral pioneer neurons (with associated glia) required for follower axon guidance into the nerve ring (Rapti et al., 2017; Zallen et al., 1998, 1999). This recurring theme suggests that the pathways governing neuroblast movements may also function to guide axons later in development.

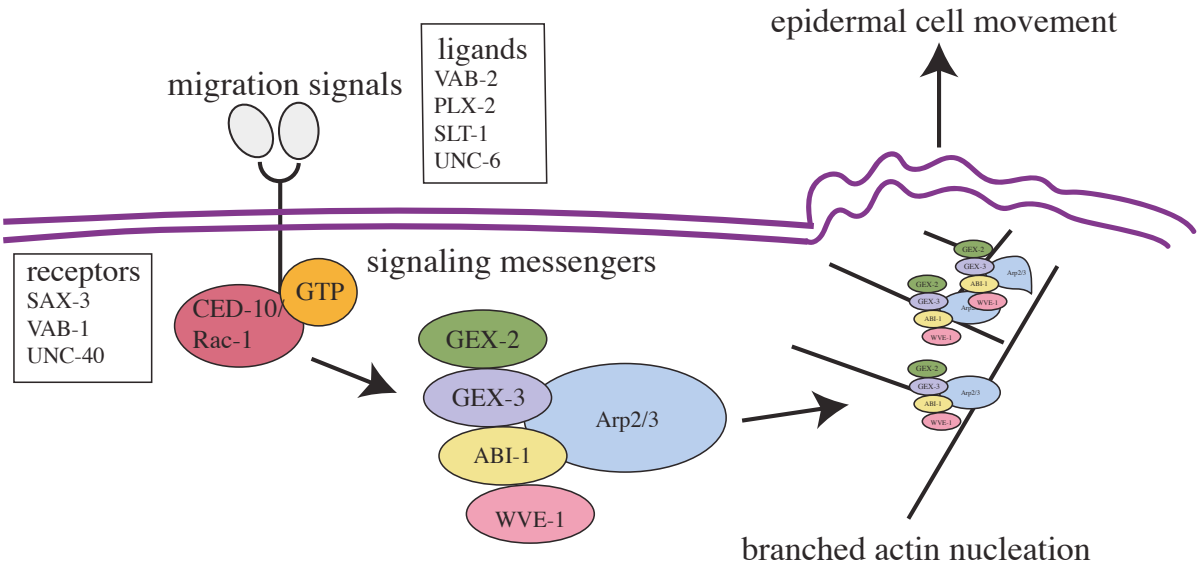

Figure 5. Ephrin, Robo, netrin and semaphorin signaling regulate epidermal cell migration during ventral enclosure. Cell migration occurs in response to cues that regulate the generation of branched F-actin to generate protrusions and/or lamellipodia that facilitates movement over a substrate. During *C. elegans* ventral enclosure, several ligands and receptors have been shown to regulate migration of ventral epidermal cells to enclose the embryo in a layer of epidermis. These receptors activate CED-10/RAC-1 to form active WASp, WAVE/SCAR complexes that in turn activate Arp2/3 to generate branched F-actin at the leading edge. Figure adapted by Patel et al., 2008 and Bernadskaya et al., 2012.

1.3.2 Signaling for neuronal development

Other signaling pathways also control neuronal cell positioning and axon guidance. Developing neuronal cells encounter signals that inform their outgrowth and polarization (Ackley, 2014). Wnt proteins are secreted, lipid-modified glycoproteins that function as signaling molecules (Zecca et al., 1996). As a secreted Wnt ligand diffuses away from its source, a gradient is formed that can be sensed by cells to receive positional information. Wnts can function as either attractants or repellents, and in *C. elegans* have been implicated in asymmetric cell division, neuronal polarity, axon outgrowth, and synaptogenesis (Ackley, 2014). Canonical Wnt ligands bind to Frizzled receptors, leading to the stabilization of β-catenin, which then regulates the expression of target genes often required for division or survival (Korswagen, 2002). Non-canonical Wnt ligands bind to Frizzled receptors, which associates with Disheveled to regulate cytoskeletal components required for migration and/or planar cell polarity (Sharma et al., 2018). In *C. elegans,* components of the non-canonical pathway have been shown to regulate axon guidance along the anteroposterior axis (Ackley, 2014). For example, *cwn-2, cfz-2* and *mig-1* are required for the anterior-posterior outgrowth of RMED/V neurites, while *mom-5, cam-1, vang-1* and *prkl-1* regulate the anterior migration of QR neuroblast descendants during different stages of development (Mentink et al., 2014; Song et al., 2010).

The amphids also interpret guidance cues for their development. The amphids are a pair of bilaterally located sensilla in the head containing sensory neurons with dendrites that protrude through a glial channel at the nose to sense cues from the outside world. Each amphid contains 12 sensory neurons, one sheath cell and one socket cell. Like other sensory neurons, each neuron in the amphid extends an axon into the nerve ring, but they also have a single dendrite to the outermost anterior of the embryo (Low et al., 2019). In contrast to other neuronal migrations,

amphid movements do not utilize long-range guidance cues. The Bao lab reported in 2019 that during dendritic extension, the amphid neurons first assemble into a rosette with the dendritic tips at the vertex, marked by the polarity protein PAR-6, and appears to attach to the epidermal cells as they migrate toward the anterior which brings the dendritic tips to a more anterior position (Fan et al., 2019). This mechanism for neuronal migration differs from the classic pioneer-follower model. Subsets of non-amphid neurons are in close proximity to the leading edge of the migrating anterior epidermal cells, and foci associated with one/both cell types are marked by PAR-6, which could indicate a similar mechanism for co-migration/dendritic extension of other neuronal cells (this study; Grimbert et al., 2021).

Subsets of neurons also internalize during mid-embryogenesis. The *C. elegans* nervous system is composed of the nerve ring, the ventral nerve cord and the main neuropil (White et al., 1986). The nerve ring, considered to be the brain, consists of a tight axon bundle that forms around the pharynx. Neurons are born throughout the embryo, and many need to undergo changes in their position to reach their final destination. Our group and the laboratory of Dr. Zhirong Bao found that subsets of neuronal cells undergo patterning through the formation of transient, planar polarity rosettes during ventral enclosure to accommodate the change in shape of the embryo from an ovoid to lengthening in the anterior-posterior axis (Fan et al., 2019; Wernike et al., 2016). In addition, our groups observed that subsets of neurons ingress into the interior of the embryo (Barnes et al., 2020; Grimbert et al., 2021). While the mechanism that mediates their ingression is not clear, the Bao lab found that HMR-1/cadherin seems to be important, and proposed that the retracting pharynx could provide the mechanical force for their involution (Barnes et al., 2020). While this model remains to be tested, prior studies showed that there is indeed force generated as the anterior

pharynx connects to the anterior, which is resisted by the apical ECM leading to the formation of a sensory depression (Portereiko & Mango, 2001).

1.4 The *C. elegans* pharynx is a model for organogenesis

1.4.1 Pharyngeal Development

The pharynx is a bilobed linear tube encased in a basement membrane that connects to the intestine at the posterior end. It is composed of the buccal cavity, the procorpus, metacorpus, isthmus, terminal bulb, and pharyngeal intestinal valve (Mango, 2007). Cells are committed to pharyngeal fate by the transcription factor PHA-4/FoxA. Pharyngeal development is robust as the pharynx has been shown to continue to develop in embryos that have arrested due to failures in epidermal morphogenesis (Ahnn & Fire, 1994; Chanal & Labouesse, 1997). Despite this autonomy, a small portion of the anterior pharynx develops separately from the rest of the pharynx and needs to be properly positioned to epithelialize and form a contiguous lumen (Figure 6).

During development, the posterior pharyngeal cells polarize to form a cyst, which defines the location of the pharyngeal lumen. These cells have apically localized PAR-3 and undergo apical constriction to form a large, stable apical rosette (Rasmussen et al., 2012). The extracellular matrix component laminin (LAM-1) orients the polarity of the cells to align the future lumen with the developing intestine at the posterior (Rasmussen et al., 2012). Our lab recently reported a second, more anterior stable rosette composed of a subset of arcade cells of the pharynx (this study; Grimbert et al., 2021). This rosette marks the site of the future mouth and anterior lumen.

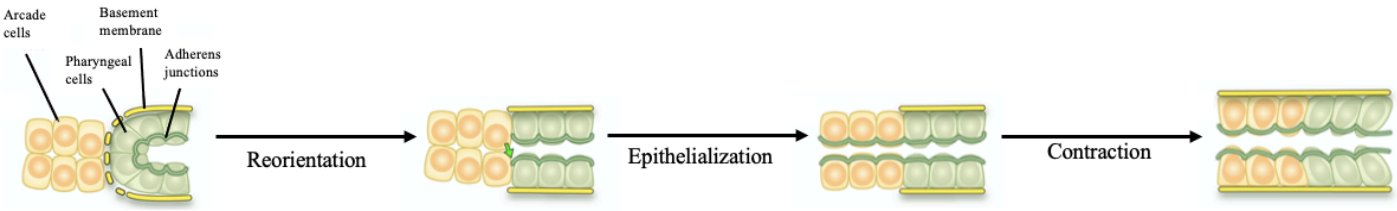

Figure 6. Anterior pharyngeal morphogenesis. A schematic shows early pharyngeal development where the arcade cells (yellow) of the anterior pharynx are progressively polarized to align with the rest of the pharynx (green). Initially, the arcade cells are not polarized, while the posterior cells have established polarity with adherens junctions. The arcade cells subsequently reorient and then begin to polarize to align and form a contiguous lumen with the pharynx. Polarization is completed as contraction generates force causing the anterior pharynx to move inward. Figure adapted from Mango, S. E., 2007.

The arcade cells at the anterior lie outside the pharyngeal basement membrane (Figure 6; Mango et al., 1994). Arcade cells connect the buccal cavity and external epidermis to the developing pharynx. After the posterior pharyngeal primordium rearranges to form a short tube of epithelial cells, the arcade cells subsequently polarize and form adherens junctions connecting them to each other, and subsequently to the rest of the pharynx (Figure 6). The gene *pha-1* is required for successful pharyngeal epithelization and anterior attachment, but the mechanism is not clear (Kuzmanov et al., 2014). In the majority of *pha-1* loss-of-function or null mutant embryos, the anterior arcade cells fail to reorient themselves and connect to the pharynx, and the pharyngeal primordium develops into a sac confined to the center of the embryo (Portereiko & Mango, 2001). The cytokinesis proteins ZEN-4 (MKLP1, kinesin) and CYK-4 (RacGAP) are also required for arcade cell polarization (Portereiko et al., 2004). These proteins form a heterotetrametric complex, also referred to as centralspindlin, that is required for microtubule bundling (Mishima et al., 2002). In metazoans, centralspindlin helps to form the central spindle, antiparallel bundled microtubules that arise between the segregating chromosomes, and activate the RhoGEF Ect2 to generate active RhoA for contractile ring assembly (Yuce et al., 2005). In *C. elegans*, *cyk-4* or *zen-4* mutant embryos have cytokinesis defects (Jantsch-Plunger et al., 2000), but the upshift of embryos with temperature sensitive alleles during mid-embryogenesis causes arcade cell defects (Portereiko et al., 2004). Specifically, the upshifted mutant embryos lack a defined arcade cell epithelium that links the pharynx to the outer epidermis (Portereiko et al., 2004). Arcade cells are still present in weak loss-of-function *zen-4* mutant embryos, however polarity markers such as PAR-3 and PKC-3 fail to accumulate (Portereiko et al., 2004). The lack of adhesion junctions (AJs) in these mutants suggests that Rho signaling may play a role in arcade cell polarization. Importantly, these findings also show that cooperation between the arcade cells

and the anterior epidermal cells is essential for proper development of the anterior lumen. However, how these cells are coordinated to give rise to a lumen at the correct time and place is not known.

1.5. Summary

Anterior morphogenesis requires the coordination of at least three tissue types and has not been previously studied. Chemical and/or mechanical signaling between subsets of neuroblasts and the overlying epidermal cells is required for ventral enclosure, which occurs prior to anterior morphogenesis and presumably could involve similar pathways (Bernadskaya et al., 2012; Chin-Sang et al., 1999; Fotopoulos et al., 2013; Ghenea et al., 2005; Ikegami et al., 2012; Patel et al., 2008; Wernike et al., 2016). Because ventral enclosure precedes and overlaps with anterior morphogenesis, we hypothesize that these pathways also govern neuroblast position and epidermal cell migrations required for anterior morphogenesis. Recent studies showed that the amphid neurons are mechanically coupled to the epidermal cells and co-migrate toward the anterior (Fan et al., 2019). Finally, other studies showed that the arcade cells polarize and attach to the anterior to form the buccal cavity, but it is not clear how these cells are positioned (Kuzmanov et al., 2014; Portereiko et al., 2004). Here, we characterize three tissue types during anterior morphogenesis: the neuroblasts, pharynx and epidermal cells. We found that the pharyngeal arcade cells undergo apical constriction to form a stable rosette where the vertex marks the site of the future lumen, and this rosette is positioned anterior to and in line with the posterior pharyngeal rosette. We also found that epidermal cell migration tightly correlates with the position of subsets of polarized neuroblasts, demarcated by projections enriched in PAR-6. To determine the mechanisms underlying these patterns and cell movements, we screened some of the different chemical

signaling pathway components and found that the Slit/Robo pathway is required for anterior morphogenesis. Our findings will be impactful for the field of developmental biology, as the mechanisms coordinating cell patterning for the morphogenesis of complex structures derived from multiple tissues are generally conserved among metazoans.

CHAPTER 2
Materials & Methods

2.1. Strain Maintenance

Worm strains were maintained as per standard protocol (Brenner, 1974). Worms were plated on nematode growth media (NGM) plates made by combining 50 mM NaCl, 50 mM Agar, 2.5 M BactoPeptone (nitrogen content 13%) in 1 L of distilled water, and after autoclaving and cooling to 55°C, 1 mM $CaCl_2$, 1 mM $MgSO_4$, 5 µg/mL cholesterol solution, and 25 mM potassium phosphate buffer (from Bioshop) was added. Approximately 14 mL was added per 6 cm culture dish, and after the plates solidified, they were plated with 100 uL *E. coli* (OP50). Approximately 3-5 adult hermaphrodites were placed on fresh plates to maintain stocks, which were kept at 20°C.

Table 1. Strains used in this study.

UM463	*cpIs42[mex-5p::mNeonGreen::PLCδ-PH::tbb-2 3'UTR, unc-119(+)] II; ItIs37[unc-119(+), Ppie-1::mCherry::HIS-58] IV*
SM481	*pxIs10 [pha-4::GFP::CAAX + (pRF4) rol-6(su1006)]*
UM456	*cpSi20[Pmex-5::TAGRFPT::PH::tbb-2 3'UTR; unc-119 (+)] I; unc-119(ed3) III*
ML916	*mcIs40 [lin-26p::ABDvab-10::mCherry+myo-2p::GFP]*
FT1197	*unc-119(ed3) III; xnIs449 [lin-26::LifeAct::GFP + unc-119(+)]*
LP216	*par-6(cp45[par-6::mNeonGreen::3xFlag + LoxP unc-119(+) LoxP]) I; unc-119(ed3) III*
LP162	*nmy-2(cp13[nmy-2::GFP + LoxP]) I*
MDX29	*ani-1(mon7[mNeonGreen^3xFlag::ani-1]) III*
AJP100	*mcIs40 [lin-26p::ABDvab-10::mCherry+myo-2p::GFP]; par-6(cp45[par-6::mNeonGreen::3xFlag + LoxP unc-119(+) LoxP]) I; unc-119(ed3) III*

AJP104	*pxIs10 [pha-4::GFP::CAAX + (pRF4) rol-6(su1006)]; unc-119(ed3) III; xnIs449 [lin-26::LifeAct::GFP + unc-119(+)]; cpIs56 [mex-5p::TagRFP-T::PLC(delta)-PH::tbb-2 3'UTR + unc-119 (+)] II*
TU3335	*uls57[unc-119p::YFP + unc-119p::sid-1+ mec-6p::mec-6]*
LP244	*par-6(cp60[par-6::mKate2::3xMyc + LoxP unc-119(+) LoxP]) I; unc-119(ed3) III*
AJP105	*uls57[unc-119p::YFP + unc-119p::sid-1+ mec-6p::mec-6]; par-6(cp60[par-6::mKate2::3xMyc + LoxP unc-119(+) LoxP]) I; unc-119(ed3) III*
AJP106	*pxIs10 [pha-4::GFP::CAAX + (pRF4) rol-6(su1006)]; par-6(cp60[par-6::mKate2::3xMyc + LoxP unc-119(+) LoxP]) I; unc-119(ed3) III*
pGR71	*hsls391[Pmir-228::myristoylated-GFP; lin-15(+)]*
OH9729	*otls302[Plsy-6::GFP; Pelt-2::RFP] lin-15(n744); nsEx4011[Phlh-16::GFP::myristoylated-GFP::UTR (pGR133); lin-15(+)]*
AJP107	*lin-15(n744); nsEx4011[Phlh-16::GFP::myristoylated-GFP::UTR (pGR133); lin-15(þ)];par-6(cp60[par-6::mKate2::3xMyc þ LoxP unc-119(þ) LoxP]) I; unc-119(ed3) III*
AJP108	*hsls391[Pmir-228::myristoylated-GFP; lin-15(þ)]; par-6(cp60[par-6::mKate2::3xMyc þ LoxP unc-119(þ) LoxP]) I; unc-119(ed3) III*

2.2. Genetic Crosses

Some of the strains in Table 1 were generated in this study by performing genetic crosses. L4-staged hermaphrodites were upshifted to 30°C for 4-5 hours, then returned to 20°C to recover and lay eggs. Heat stress induces the formation of null X gametes to give rise to males. L4 males (10-12) were collected from the heat-shocked plates and added to mating plates (NGM with a small drop of OP50) with two L4 hermaphrodites from the other strain. After progeny were produced, they were single-picked onto separate plates and selfed to screen for the desired genotype. The number of single worms picked for subsequent screening varied depending on the number of loci involved in the cross.

2.3. RNA Interference

RNA interference (RNAi) was accomplished according to Kamath et al. (2001) by feeding worms *E. coli* (HT115) transformed with L4440 vector containing cDNA for a specific target. The vector contains IPTG-inducible promoters (T7) on each strand to make dsRNA. The vector also contains an ampicillin cassette for selection. In *C. elegans*, longer dsRNA molecules are used to trigger an RNAi response. Since *C. elegans* feeds on bacteria as a food source, they eat the bacteria induced to express dsRNA, which is subsequently transported across the gut cells and into the germline.

Frozen stocks of *E. coli* transformed with L4440 were streaked out on ampicillin plates and grown overnight at 37°C. A single colony was picked and cultured overnight in 5 mL LB Amp media (5g yeast extract, 17 mM NaCl, 10M tryptone in 1 L of distilled water) and 5 μL of 100 mg/mL ampicillin (Amp) stock. The next day, 5 mL of LB Amp was inoculated with 50 μL of the overnight culture and incubated for six to seven hours until the O.D. was between 0.6-1.0. The cultures where then centrifuged and resuspended in fresh LB Amp (100 – 400 μL; typically range, which changed depending on the dsRNA and desired strength) and plated on NGM plates containing 50 mg/mL ampicillin and 1 mM IPTG. Approximately 15 L4-stage hermaphrodites were placed onto each RNAi plate and kept for 24-48 hours at 20°C before live imaging. For the analysis of phenotypes after *pha-4* RNAi, worms were incubated for 24 hours, while they were only incubated for 3 hours for the analysis of phenotypes after *zen-4* RNAi. The Y49E10.19 (*ani-1* RNAi), M03D4.1 (*zen-4* RNAi) and F38A6 (*pha-4* RNAi) clones used in this study were generously provided by J. C. Labbe (IRIC, Montreal, QC) and Michael Glotzer (University of Chicago, Chicago, IL).

2.4. Microscopy

Live imaging was performed on embryos. Embryos were collected directly from the plate or by cutting a hermaphrodite adult worm in approximately 20 μL of M9 liquid (40 mM disodium phosphate, 22 mM monopotassium phosphate, 85 mM sodium chloride and 2 mM magnesium sulfate) in a depression slide. The embryos were then transferred onto an agarose gel pad on a glass slide containing a piece of silicone. The agarose was prepared by heating 0.08 g of agarose in 4 mL of water for 30 seconds. A drop of agarose solution was placed onto a slide with silicone and covered by a second slide until the agarose dried. Finally, a coverslip was added to seal the agarose pad between the glass slide.

Most imaging was done using an inverted Nikon Eclipse Ti microscope outfitted with the Livescan Sweptfield scanner (Nikon), Piezo Z stage (Prior), an Andor IXON 897 EMCCD camera using the 488 and 561 nm lasers. Images were collected with the 100x/1.45 NA objective using NIS Elements (Nikon) acquisition software. Z-stacks of 0.5 μm (~20) were collected at 2-minute intervals starting from the onset of ventral enclosure until twitching (2-fold). Embryos were filmed from a ventral view and the appropriate Z stack was chosen to be slightly less then midway through the embryo away from the coverslip to capture both cortical localization and the midplane. Other embryos were moved with an eyelash to be en face (anterior up), and Z stacks were chosen from midway/posterior pharynx – coverslip/epidermis.

Screening of the embryos for the genetic crosses was done using the LEICA DMI6000B microscope with the 40X/1.25 NA objective, Hamamatsu Orca R2 camera, piezo Z/ASI stage (MadCityLab), and Volocity acquisition software (PerkinElmer).

Highly inclined and laminated optical sheet (HILO), modified total internal reflection fluorescence (TIRF) imaging, was performed using an inverted Nikon Ti-E microscope outfitted with a NI-DAQ piezo Z stage (National Instruments), and an Evolve (EMCCD) camera using the 488 and 561 laser diodes, and a 100x CFI Apo TIRF objective with Elements 4.0 acquisition software (Nikon). Images were exported as TIFFs and opened in Image J (NIH Image) to create Z-stack projections, perform image rotation and to crop desired regions.

2.5. Image Analysis

Time-lapse movies were deconvolved using AutoQuant X3 (MediaCybernetics). Files were opened with metadata and deconvolved using adaptive (theoretical) PSF (blind deconvolution). The total number of iterations varied from 5-10 and the noise level was set to medium or high depending on the intensity of the fluorescent signal and the background. Deconvolved images were imported into IMARIS 7.7.2 (Bitplane) and 3D surface rendering was applied equally on Z-stack projections All measurements were performed in Image J (NIH Image) or Fiji.

CHAPTER 3

Results

3.1 Characterizing cell patterns during anterior morphogenesis

Since little was known about anterior morphogenesis prior to our work, my colleagues first set out to characterize the cell movements that occur during this developmental stage. To do this, they visualized all cells in *C. elegans* embryos co-expressing a marker for the membrane (mNeonGreen::PH) and chromatin (H2B::mCherry) using sweptfield confocal microscopy (n = 37). Filming the embryos head-on revealed that cells organize at the anterior by forming a ring within a ring, where the centre of the ring marks the site of the future lumen (Figure 7; *en face* view). The cells in the inner ring, which are likely neuroblasts, ingress into the embryo (Figure 7), while the overlying cells, which are likely hypodermis (epidermal cells), encircle the site of the future lumen. Next, we determined which cell types contribute to anterior morphogenesis, and the specific patterns associated with these cells.

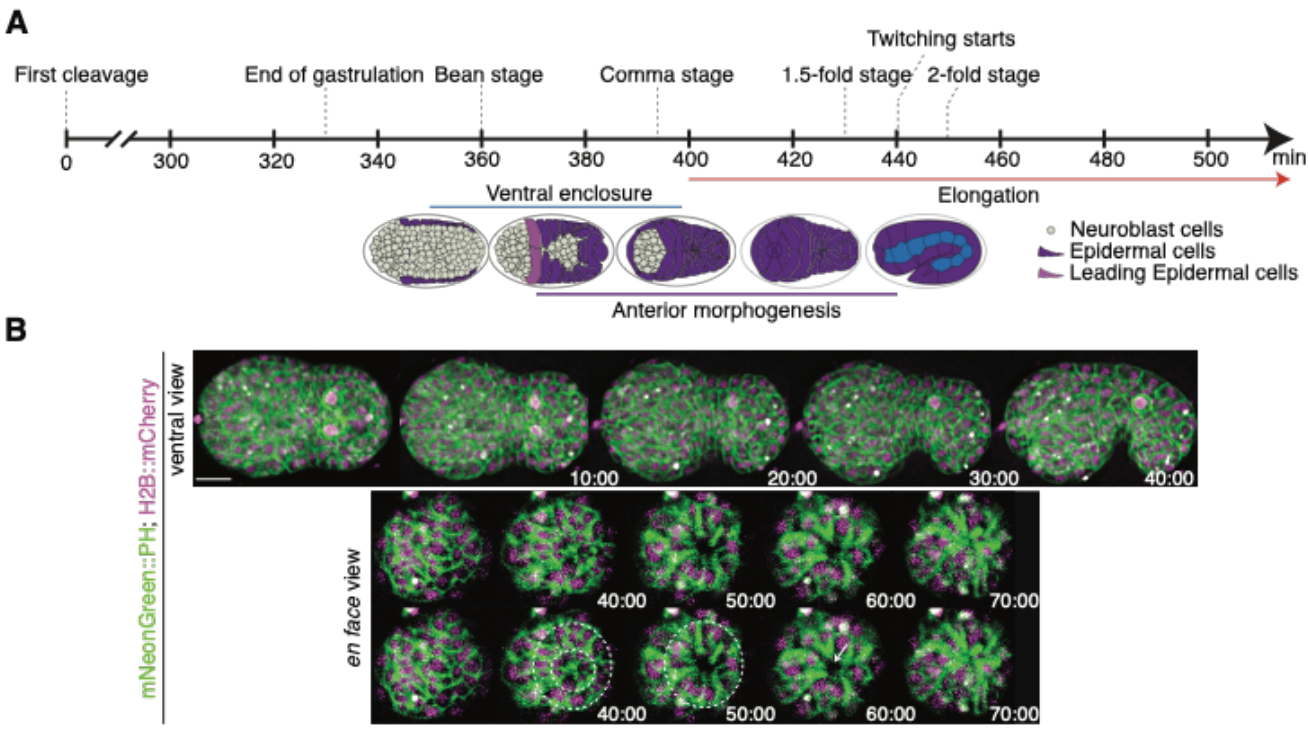

Figure 7. Cells ingress during anterior morphogenesis. A) The timeline (in minutes) shows the key morphogenetic events that occur during *C. elegans* embryogenesis. Anterior morphogenesis begins when the leading pair of migrating epidermal cells meet at the ventral midline (t = ~380) and continues throughout ventral enclosure and part of elongation (~440 minutes/twitching stage). **B)** Time-lapse images obtained by sweptfield microscopy (ventral view; anterior to the left) show an embryo co-expressing mNeonGreen::PH to visualize membranes (green) and H2B::mCherry to visualize nuclei (magenta) through anterior morphogenesis (time in minutes). The *en face* view shows cell organization at the anterior of the embryo, which results in the formation of a 'ring in a ring' (white dashed circles). The star-like pattern in the center marks the site of the future lumen, which forms after cells ingress into the embryo. Times are shown in minutes, and the scale bar is 10 μm. Figure adapted from Grimbert et al., 2021.

3.2 The arcade cells polarize and form a rosette during anterior morphogenesis

Next, we determined the patterns formed by the pharyngeal tissue during anterior morphogenesis. Embryos expressing a marker for the pharyngeal cell fate determinant PHA-4 tethered to the membrane (PHA-4::GFP::CAAX), and a membrane marker for all cells (TagRFP::PH) were imaged during anterior morphogenesis (n = 18). At the beginning of anterior morphogenesis, the arcade cells formed projections that pointed toward the anterior of the embryo and remained in place for an extended period of time (Figure 8A). Filming embryos with a head on view revealed that 6 arcade cells formed a stable rosette (n = 13, Figure 8B). The cells formed a tear-drop-like shape, and the tips of the cells came together to form a point that defined the site of the future lumen (Figure 8C).

To determine if the projections of the arcade cells are apically polarized structures, I imaged embryos co-expressing the fluorescently-tagged pharyngeal marker (PHA-4::GFP::CAAX) co-expressed with a fluorescently-tagged PAR-6 (PAR-6::mKate2) during anterior morphogenesis (n = 18, Figure 8D). I found that the tips of the arcade cells were indeed enriched with PAR-6, which coalesce to form a bright focal point at the site of the future lumen. This data provides further support that the arcade cells form an apical rosette.

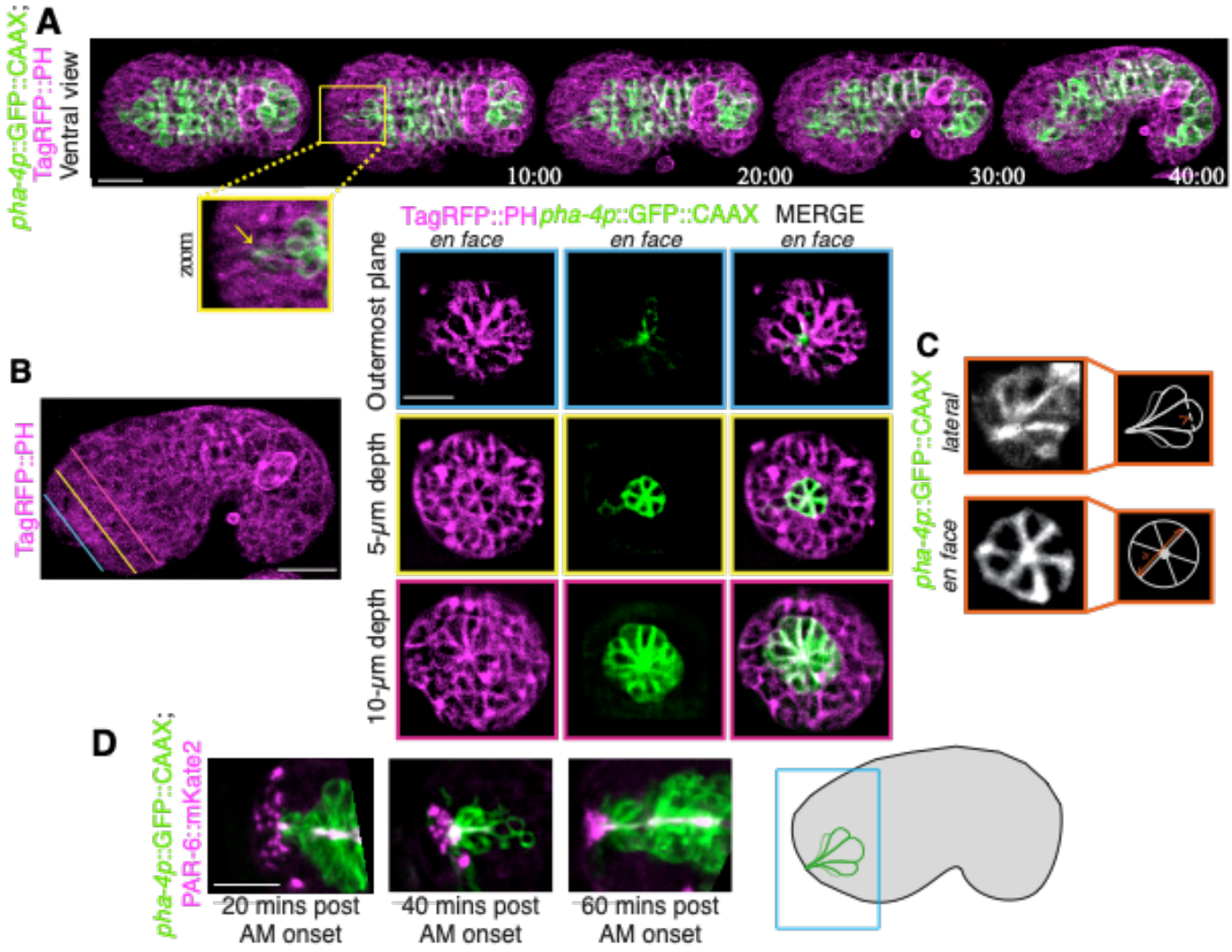

Figure 8. The pharyngeal arcade cells form a rosette. A) Time-lapse images acquired using sweptfield microscopy show an embryo co-expressing *pha-4p*::GFP::CAAX to visualize the pharyngeal cells in green and Tag-RFP::PH to visualize membranes in magenta during anterior morphogenesis. The anterior-most pharyngeal cells (arcade cells) form apical constrictions (yellow box) which coalesce (zoom; yellow arrow). Times are shown in minutes, and the scale bar is 10 μm. **B)** Images show an embryo ~ the 1.5-fold (~ 40 min) stage expressing Tag-RFP::PH to visualize membranes (magenta). The colored lines indicate the three depths in the embryo corresponding to the images to the right. Images show separate and merged channels from an

embryo co-expressing Tag-RFP::PH (magenta) and *pha-4p*::GFP::CAAX to visualize pharyngeal cells (green) at ~ 40 min. Three *en face* views are shown, which correspond to the depths (colored lines). The outermost plane (blue) shows the coalescence of the arcade-cell projections at the anterior of the embryo. At a 5 μm depth into the embryo (yellow) a small multicellular pharyngeal rosette is visible. The larger, previously characterized pharyngeal rosette is visible at a depth of 10 μm (pink). The scale bars are 10 μm. **C)** Images show *en face* or lateral views of *pha-4p*::GFP::CAAX outlining the anterior rosette. The cartoon schematics to the right show the regions used to determine the diameter and length of individual cells. **D)** Shown are images from excerpts of different time-lapse movies from embryos co-expressing PAR-6::mKate2 (magenta) and *pha-4p*::GFP::CAAX (green) acquired using sweptfield microscopy during anterior morphogenesis. The panel on the left is at ~20 minutes, the middle is at ~30 minutes, and the right is at ~40 minutes after the beginning of anterior morphogenesis (when the leading pair of ventral epidermal cells met at the ventral midline). The scale bar for each image is 10 μm. A cartoon on the right shows the relative position of the images in the embryo. Figure adapted from Grimbert et al., 2021.

Since PAR-6 could be expressed in multiple cell types, we determined if the majority of the signal within the anterior bright focal point corresponded to the pharyngeal arcade cells. To do this, I performed RNAi against PHA-4 or ZEN-4, which are required for pharyngeal cell fate and arcade cell development, respectively. If the bright focal point is composed of the tips of the pharyngeal arcade cells, disrupting the tissue should result in a decrease in signal intensity. Indeed, there was a decrease or delay in PAR-6 fluorescence at the location where the bright focal point was located, particularly during earlier stages of anterior morphogenesis (n = 7/9 for *pha-4*, and 14/15 for *zen-4*, Figure 9). However, while the signal took longer to appear and was dimmer compared control embryos, the signal did not disappear entirely, suggesting that other cell types could contribute to the PAR-6 expressing bright focal point.

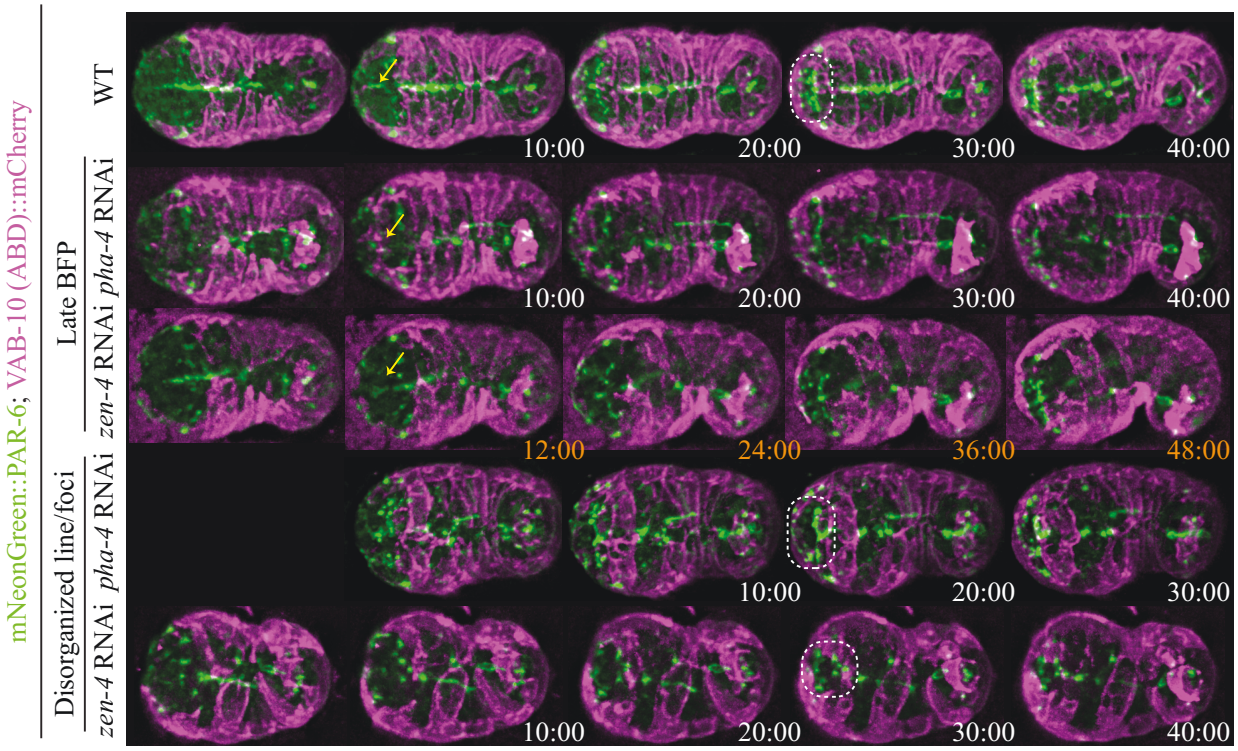

Figure 9. The arcade cells are required for anterior morphogenesis. Time-lapse images acquired using sweptfield microscopy show control (top panels), *pha-4* or *zen-4* RNAi embryos expressing mNeonGreen::PAR-6 (green) and *lin-26p*;VAB-10 (ABD)::mCherry (magenta) during anterior morphogenesis. Yellow arrows point to the position of the bright focal point (BFP), which demarcates the site of the future lumen, while the dotted circles highlight the location of the pentagon and semi-circle of foci. The times are indicated in minutes. The scale bar is 10 μm. Figure adapted from Grimbert et al., 2021.

3.3 Neuroblasts govern migration of the anterior epidermal cells

In addition to marking the tips of arcade cell projections, we observed patterns formed by PAR-6 foci in the anterior of the embryo (Figure 10A). These patterns include two pentagons on either side of the bright focal point, and a semi-circle of foci positioned ventrally to the bright focal point. The semi-circle of foci correlated tightly with the free edge of the migrating ventral epidermal cells. Time-lapse movies of embryos co-expressing mNeonGreen::PAR-6 and a marker for epidermal-specific F-actin [*lin-26p*::VAB-10 (ABD)::mCherry] revealed that epidermal F-actin projections extend towards and contact the semi-circle foci, but never pass them (n = 15; Figure 10A). The pentagons have several foci that correlate tightly with the dorsally migrating epidermal cells (two posterior-most foci), while the others likely correspond to polarized neuroblasts (remaining 3 foci of each pentagon).

To determine which of the polarized structures marked by PAR-6 correspond to neuroblasts (neuronal precursor or support cells), we filmed embryos co-expressing mKate2::PAR-6 and markers for different subsets of neurons or glial cells. Our lab previously found that ANI-1 (anillin) is expressed in the neuroblasts, but not in the epidermis or other cell types (Fotopoulos et al., 2013; Wernike et al., 2016). We found that ANI-1 localized to foci that formed pentagons similar to PAR-6 (n = 29, Figure 10B). The pan-neuronal marker UNC-119 displayed a strong correlation with several foci in the semi-circle (outer foci) and all pentagon foci, confirming that polarized neuronal tissue does contribute to the foci patterns (n = 35, Figure 10C). The pan-glial marker MIR-228 primarily correlated with the pentagon foci (n = 6), while the HLH-16 marker, which is expressed in SMDD/AIY and SIAD/SIBV neurons, correlated with some of the semi-circle of foci, but not the pentagons (n = 20, Figure 10D).

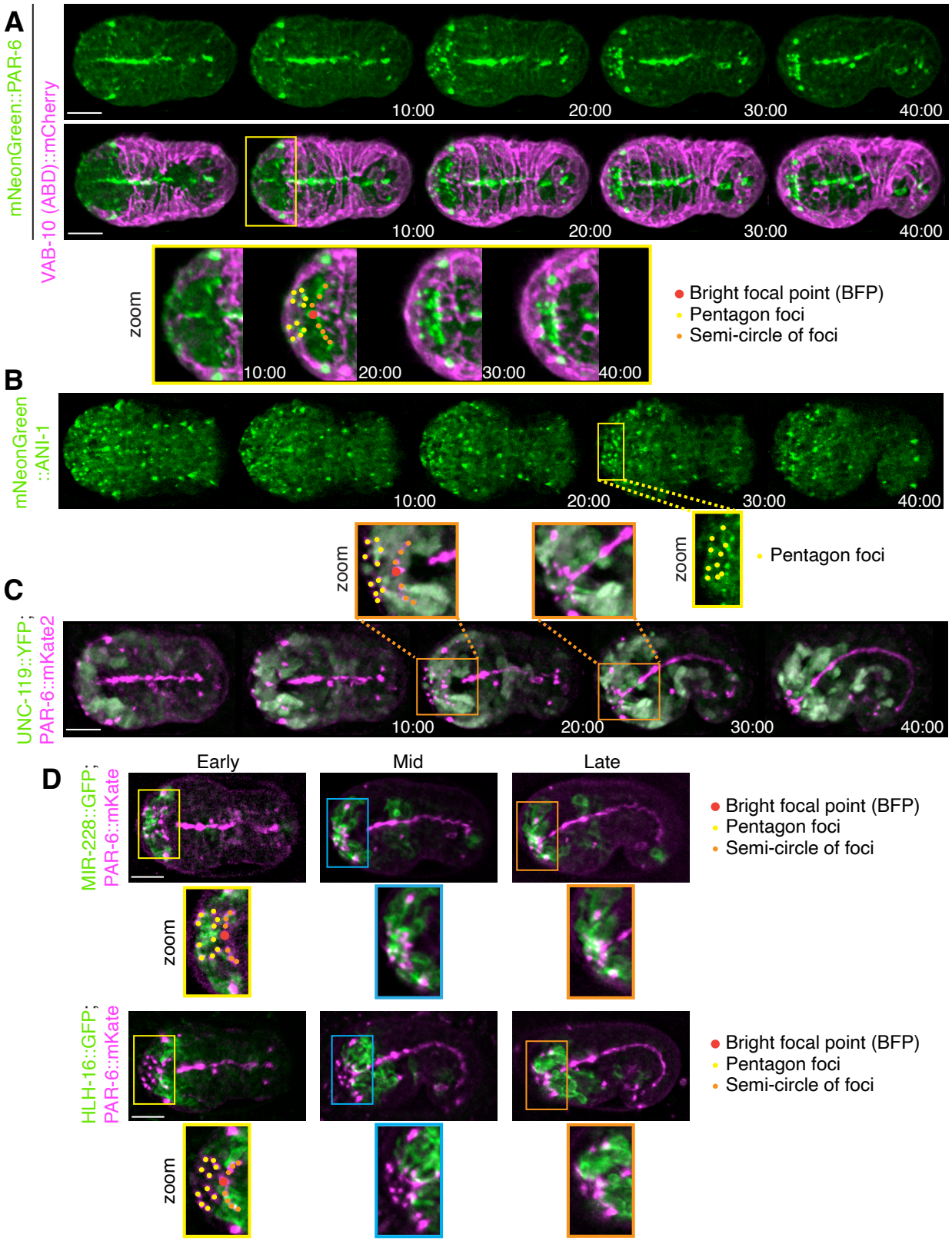
A
mNeonGreen::PAR-6
VAB-10 (ABD)::mCherry
10:00
20:00
30:00
40:00
zoom
Bright focal point (BFP)
Pentagon foci
Semi-circle of foci
B
mNeonGreen
::ANI-1
Pentagon foci
C
UNC-119::YFP;
PAR-6::mKate2
D
Early
Mid
Late
MIR-228::GFP;
PAR-6::mKate
HLH-16::GFP;
PAR-6::mKate

Figure 10. Distinct patterns formed by PAR-6 foci correlate with the migrating anterior epidermal cells. A) Time-lapse images acquired using sweptfield microscopy show ventral views of an embryo expressing mNeonGreen::PAR-6 (green; top panel) and epidermal VAB-10 (ABD)::mCherry (magenta; middle panel) during anterior morphogenesis. Times are shown in minutes, and the scale bar is 10 μm. Zoomed-in regions (bottom panel; 200%) show the patterns formed by PAR-6 more clearly (yellow box). PAR-6 localizes to the BFP (zoom; red), the pentagon foci (zoom; yellow), and the semi-circle of foci that corresponds to the anterior-most boundary of ventral epidermal cells (zoom; orange). **B)** Time-lapse images acquired using sweptfield microscopy show ventral views of embryos expressing mNeonGreen::ANI-1 (green). Times are shown in minutes, and the scale bar is 10 μm. Zoomed-in regions (yellow box; 150%) show the patterns in the anterior region more clearly. **C)** Time-lapse images acquired using sweptfield microscopy show embryos expressing UNC-119::YFP (green) and PAR-6::mKate2 (magenta). Times are shown in minutes, and the scale bar is 10 μm. Zoomed-in regions (orange box; 150%) show the neuronal projections in the anterior region more clearly. **D)** Images acquired using sweptfield microscopy show embryos expressing MIR-228::GFP (top; green) or HLH-16::GFP (bottom; green) and PAR-6::mKate2 (magenta) during early, mid or late stages of anterior morphogenesis. Times are shown in minutes, and the scale bar is 10 μm. Zoomed-in regions (yellow, blue and orange boxes; 150%) show the neuronal projections in the anterior region more clearly. Figure adapted from Grimbert et al., 2021.

We wanted to better understand the contribution of the arcade cells and neuroblasts to epidermal cell migration. As shown in Figure 8, the PAR-6 bright focal point corresponds to projections from the arcade cells, but none of the other foci correspond to these or other pharyngeal cells. Depletion of *pha-4* or partial depletion of *zen-4*, which cause loss of pharyngeal cell fate or disrupts arcade cell development, respectively, caused some of the pentagon and semi-circle of foci to be disorganized, along with epidermal cell migration defects (n = 6/14 for *pha-4*, and 8/16 for *zen-4;* Figure 9). This non-autonomous effect on the epidermal and neuroblast tissue suggests that signaling associated with the arcade cells is important for positioning the surrounding neuroblasts and for epidermal cell migration.

To determine how neuroblast positioning affects epidermal cell migration, we depleted *ani-1* in embryos co-expressing mNeonGreen::PAR-6 and a membrane marker mCherry::PH (n = 34; Figure 11). Our lab previously showed that *ani-1* (anillin) is required for neuroblast cell division and is expressed primarily in the neuroblasts and not in the epidermis during embryogenesis (Fotopoulos et al., 2013). By following amphid migration, which co-migrate with the anterior epidermis, my colleagues observed delays in amphid/epidermal cell migration from mild to severe, where severely delayed embryos took more than twice the amount of time for the cells to reach the anterior compared to control embryos (Figure 11A, B). The severely delayed embryos also displayed pharyngeal polarization defects, where there was a lack of a contiguous lumen formed between the anterior and posterior pharynx (Figure 11A, B). The cell migration delay phenotypes correlated with abnormally positioned or missing pentagon or semi-circle of foci (Figure 11C).

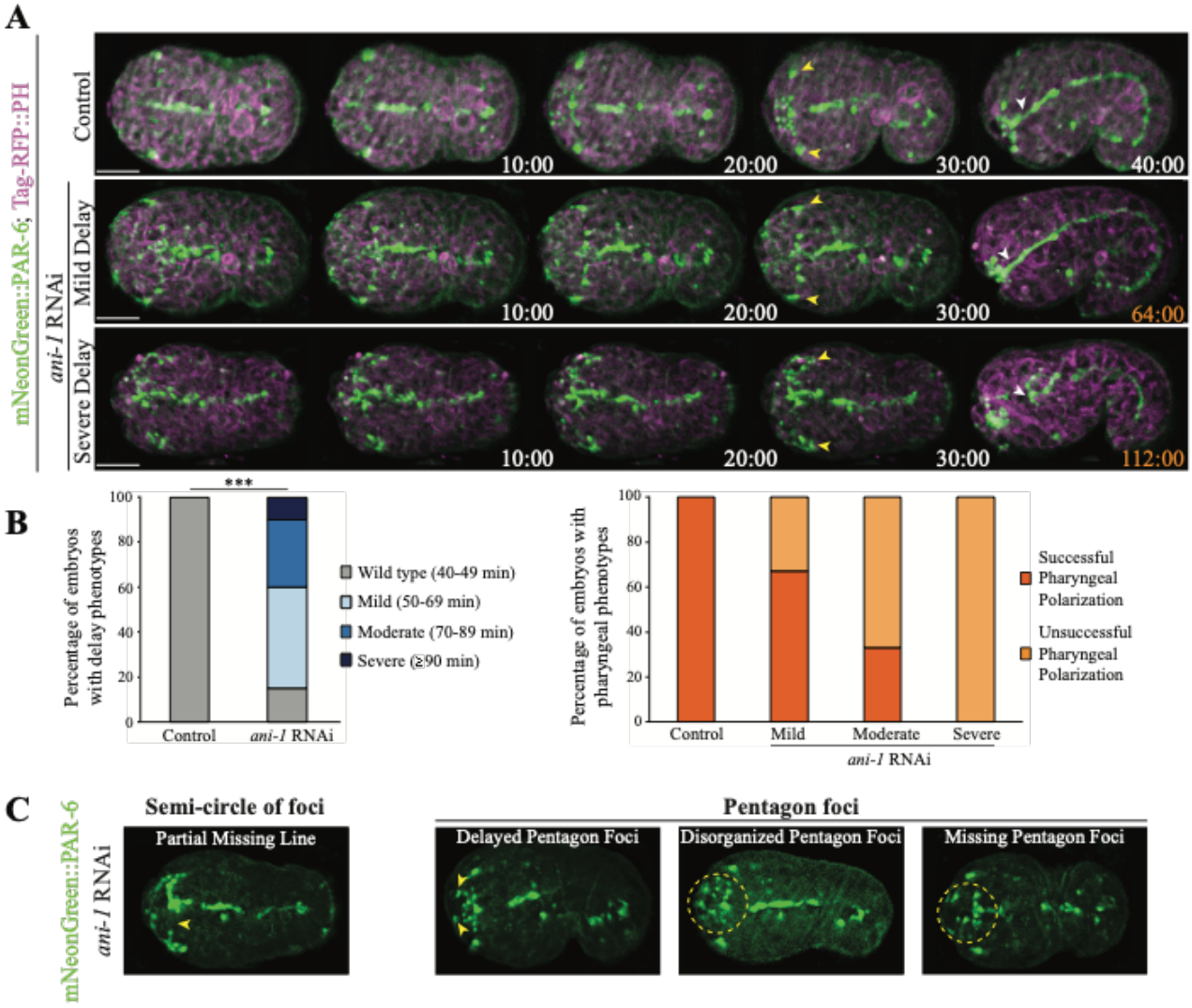

Figure 11. Disrupting neuroblast division causes delays in anterior epidermal cell migration.

A) Time-lapse images acquired using sweptfield microscopy show ventral views of embryos expressing mNeonGreen::PAR-6 (green); Tag-RFP::PH (magenta) in control (top panel) and after *ani-1* RNAi to disrupt neuroblast cell division (middle and bottom panels). Delays in epidermal cell migration, marked by the amphid dendrites (yellow arrowheads), correlated with changes in the number or position of PAR-6 foci and/or failure of the anterior pharynx to polarize (white arrowheads) in *ani-1*–depleted embryos compared to control embryos. **B)** Epidermal cell

migration was monitored by measuring the time it took for the amphid dendrites to reach the anterior region. The bar graph on the left shows the proportion of embryos with different delays in epidermal cell migration after *ani-1* RNAi when compared with control embryos. The bar graph on the right shows the proportion of control and *ani-1* RNAi embryos with delay phenotypes in which the anterior pharynx failed to polarize. **C)** Images show changes in the patterns of PAR-6 foci observed in mNeonGreen::PAR-6 (green) embryos with epidermal cell migration delays after *ani-1* RNAi. The scale bar for all embryos is 10 μm. Figure adapted from Grimbert et al., 2021.

To further understand how disrupting the neuroblasts affects epidermal cell migration, I used HILO (highly inclined and laminated optical sheet) microscopy to image *ani-1* depleted embryos expressing a marker for epidermal F-actin (*lin-26p*::VAB-10 (ABD)::mCherry or *lin-26p*::GFP::LifeAct; Figure 12). HILO microscopy permitted us to image embryos with high speed to visualize the epidermal cell F-actin projections, which turnover too quickly to be captured by sweptfield confocal microscopy. Counting the number of ventral epidermal cell projections over time revealed a decrease in the *ani-1* depleted embryos compared to control ($n = 6$ for control, and 8 for *ani-1* RNAi; Figure 12). This finding suggests that neuroblast number and/or position is required for the proper formation of F-actin projections in the ventral epidermal cells, which likely impacts their migration.

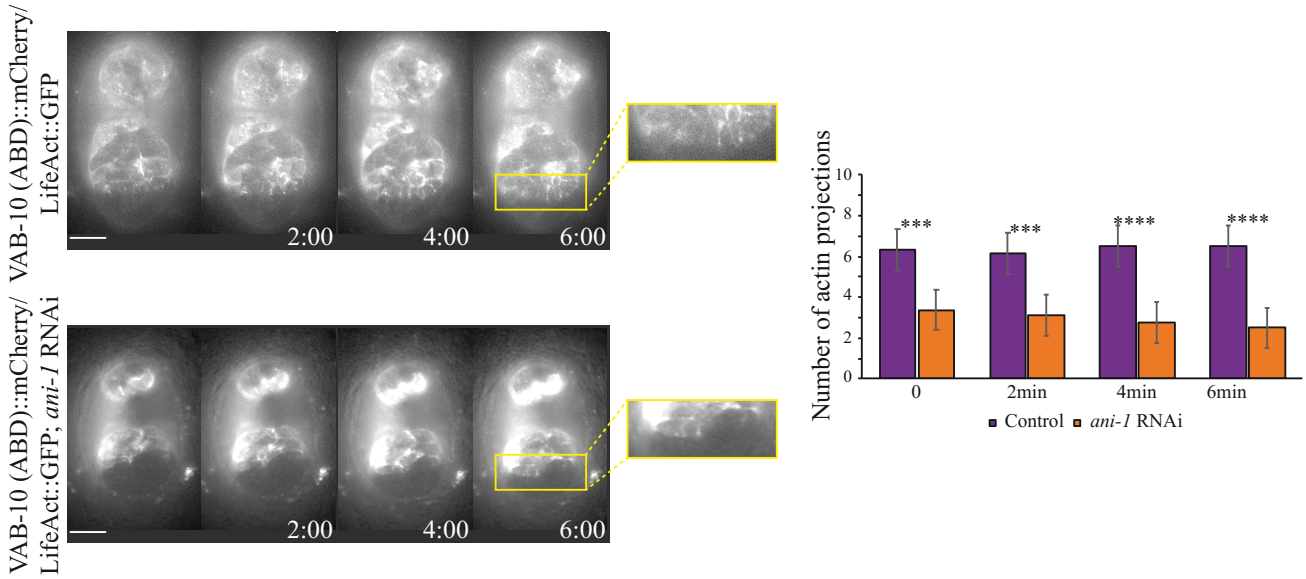

Figure 12. Neuroblasts are required for the F-actin rich ventral epidermal cell projections. Time-lapse images acquired by HILO microscopy show ventral views of control or *ani-1* RNAi embryos expressing epidermal LifeAct::GFP or VAB-10 (ABD)::mCherry in greyscale. Zoomed in regions (yellow box) show the projections more clearly. To the right, the bar graph shows the average number of projections for each time point in minutes as indicated. The asterisks indicate $p < 0.0005$.

3.4 The Slit/Robo pathway regulates anterior morphogenesis

We propose that the neuroblasts signal to the overlying anterior epidermal cells to control the formation of F-actin projections required for their migration. Several pathways have been shown to regulate ventral epidermal cell migration during ventral enclosure, and we hypothesize that one or more of these pathways similarly function during anterior morphogenesis. Using RNAi, I first depleted downstream components including *wve-1*, *wsp-1* and *gex-3* known to regulate branched F-actin, to verify that I could phenocopy the epidermal migration defects caused non-autonomously by *ani-1* RNAi. Although *wsp-1* RNAi did not give strong phenotypes, likely due to low penetrance of the RNAi, embryos depleted of *wve-1* (n = 10/22) or *gex-3* (n = 25/34) displayed anterior epidermal migration defects (Figure 13A). Interestingly, the patterns of cells expressing PAR-6 were also disrupted, including the pentagons and semi-circle of foci (Figure 13A). This supports that epidermal cells contribute to these foci in addition to polarized neuroblasts. I also observed mis-positioning of the anterior lumen, which is consistent with what we had previously observed after depletion of *elt-1*, a gene required for epidermal cell fate (data not shown).

Next, I screened several ligands for different pathways that could control cytoskeletal regulation including Wnt (*cfz-2*, *mom-5*), plexin (*plx-2*) and slit (*slt-1*), and I observed cell patterning and anterior morphogenesis defects after *slt-1* depletion (n = 6/22; Figure 13A). Several of the *slt-1* RNAi embryos also failed during ventral enclosure, which had not been previously reported (n = 4/22). Next, I depleted the Slit receptor, Robo (*sax-3*) and similarly observed foci patterning and morphogenesis defects (n = 5/43; Figure 13A). I found that similar to *ani-1* RNAi, there was a range of anterior epidermal migration phenotypes in *slt-1* and *sax-3* RNAi embryos with increasing severity from mild (no/short delay), to moderate (delays of 50-69 minutes) and

severe (>70 minutes; Figure 13B, C). This evidence suggests that the Slit/Robo pathway controls epidermal cell migration during anterior morphogenesis.

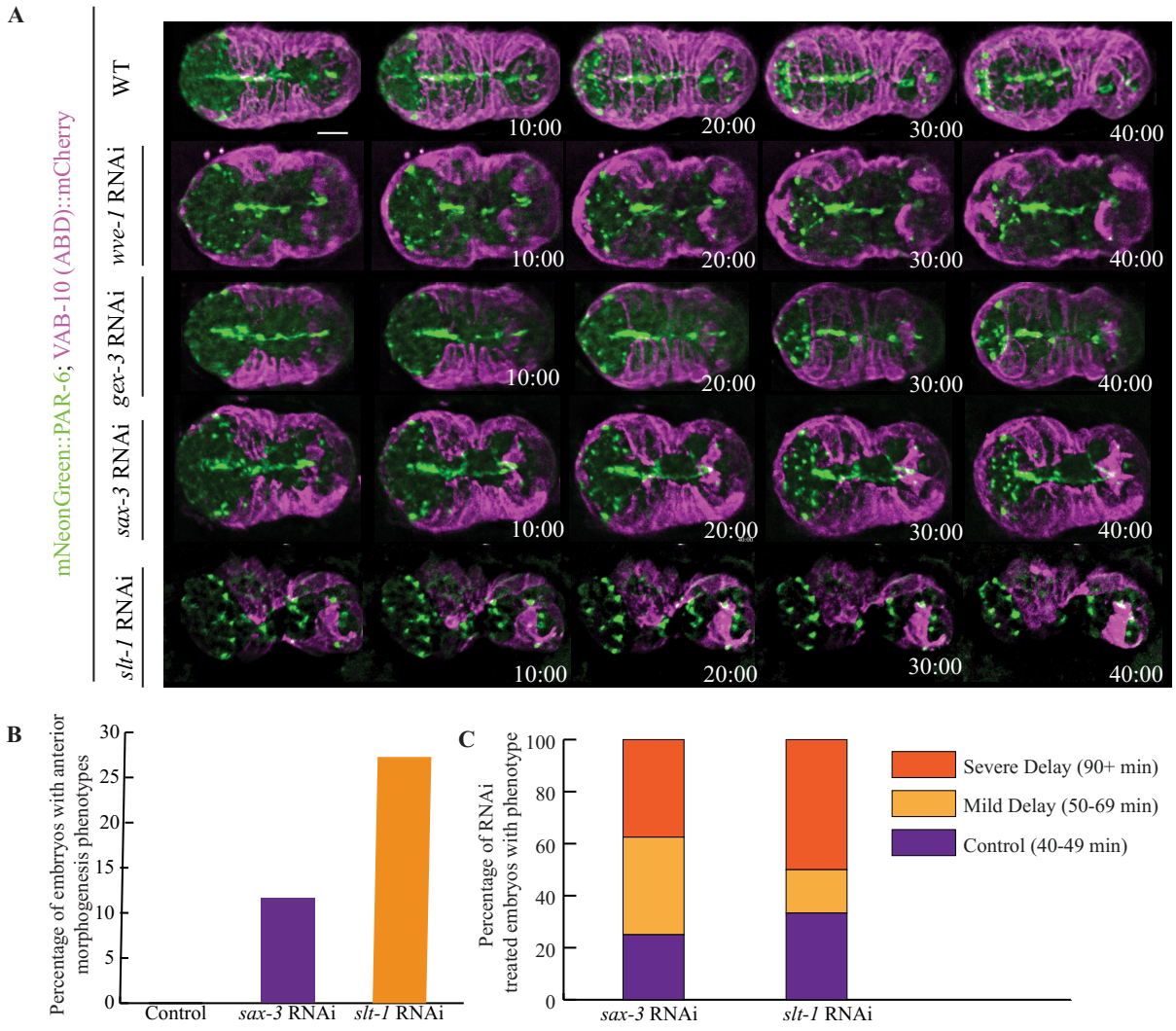

Figure 13. The Slit-Robo pathway regulates epidermal cell migration for anterior morphogenesis. **A)** Time-lapse images show control, *wve-1*, *gex-3*, *sax-3* and *slt-1* RNAi embryos co-expressing mNeonGreen::PAR-6 (green) and epidermal F-actin [VAB-10::(ABD)::mCherry; magenta]. Times are shown in minutes and the scale bar is 10 µm. **B)** A bar graph shows the proportion of embryos with anterior morphogenesis defects in *sax-3* and *slt-1* RNAi embryos compared to control embryos. **C)** Bar graphs showing the proportion of epidermal migration phenotypes with different severities in the *sax-3* and *slt-1* RNAi effected embryos.

CHAPTER 4
Discussion

Our work pioneered the characterization of anterior morphogenesis. Neuronal, pharyngeal, and epidermal tissues must be spatiotemporally coordinated for development of the anterior lumen. Using different types of microscopy and cell-specific markers we revealed the different movements and patterns formed by these three cell types, and their interdependence for proper lumen formation. Specifically, polarized structures enriched with the polarity protein PAR-6 revealed striking patterns of foci associated with pharyngeal, neuronal and epidermal cells. The tips of six arcade cells enriched with PAR-6 form a visibly bright focal point which marks the site of the future lumen. The highly polarized tips of neuroblast cells extend projections that associate with PAR-6 positive polarized structures that form the two pentagon foci and a semi-circle of foci. Similarly, the migrating epidermal cells polarize to extend projections that associate with several pentagon foci and the semi-circle of foci. Although not fully understood, the patterns observed from the PAR-6 polarized structures may reveal a mechanical cue of adhesion molecules that provide a mechanism for controlling dorsal and ventral epidermal cell migration during anterior morphogenesis. Disrupting the pharyngeal cells or neuronal cells caused epidermal cell migration phenotypes demonstrating the requirement of these tissues and their non-autonomous roles in anterior morphogenesis. In support of this, we discovered a role for the Slit-Robo pathway, typically required for neuronal cell development, in regulating anterior epidermal cell migration.

Our studies found that the arcade cells in the anterior pharynx form a stable rosette that demarcates the future lumen. We found that soon after the onset of anterior morphogenesis, six of the arcade cells polarize and form apical constrictions to give rise to a teardrop-like shape. These cells form a stable rosette, and their tips mark the site of the future lumen, visualized by the polarity

protein PAR-6 (bright focal point; Figure 8). The anterior rosette is in line with the previously characterized posterior rosette, formed by a large number of pharyngeal cells. In addition to using a membrane-tethered fate-determinant marker to outline the pharyngeal cells, we performed *pha-4* and *zen-4* RNAi to show that the pharyngeal and arcade cells, respectively, contribute to the PAR-6 bright focal point. Interestingly, a delayed weaker signal arose later in anterior morphogenesis suggesting that the knockdown was either not complete, or that other cell types could contribute to this signal. Further, we observed disorganization of the other foci (pentagons and semi-circle of foci). These findings suggest that the bright focal point contributed by pharyngeal cells plays a role in regulating the surrounding tissues for proper anterior lumen formation and development of the anterior region.

The contribution of neuronal tissue to the other foci patterns was characterized by co-localization of different neuronal or glial markers with PAR-6. The pan-neuronal and support cell marker UNC-119 revealed striking projections that extended to the pentagons and some of the semi-circle foci (Figure 10). The pan-glial marker MIR-228 also showed strong correlation with the pentagon foci. This was expected, as at this early stage of neuronal development, glia are present at the anterior of the embryo where they act as guide posts for neuronal outgrowth. Lastly, HLH-16::GFP, which is expressed in a subset of neurons, correlated with some of the semi-circle of foci. Importantly, the F-actin projections from the anterior ventral epidermal cells also strongly correlate with the semi-circle of foci and never cross this line. Therefore, multiple neuronal and glial cell types could be involved in signaling to the epidermal cells to control their migration.

In support of a role for the neuroblasts in controlling epidermal cell migration, disrupting neuroblast cell division by *ani-1* RNAi caused disorganized, missing, or delayed foci phenotypes and anterior morphogenesis defects with a range of severity. Specifically, we observed mild,

moderate and severe delays in anterior ventral epidermal cell migration. Further characterization of these phenotypes revealed that there was a decrease in the number of epidermal F-actin projections formed in *ani-1* RNAi embryos. This data shows that the neuroblasts are required for epidermal cell migration for anterior morphogenesis. The neuroblasts could signal directly to the epidermal cells through a ligand/receptor interaction, and/or some type of adhesion could arise between the two cell types, similar to the amphids, which helps cells in the two tissues to co-migrate.

To investigate the signaling pathways that govern anterior morphogenesis, I performed an RNAi screen to perturb different signaling pathways previously shown to regulate ventral enclosure and/or neuronal development in *C. elegans*. I found that the Slit/Robo pathway plays a role in regulating anterior morphogenesis. RNAi of *sax-3* (the Robo receptor) and *slt-1* (the slit ligand) caused disorganized foci, and moderate to severe delays in anterior ventral epidermal cell migration. Robo was previously shown to function in ventral enclosure in *C. elegans* and has been studied in axonal guidance in vertebrates. Interestingly, Slit was not previously shown to have a role in ventral enclosure, so this was a novel finding from our studies. A previous study showed that Robo is required for ventral enclosure, and is redundant with several other signaling pathways (Bernadskaya et al., 2012). The proportion of embryos with anterior morphogenesis phenotypes caused by *slt-1* or *sax-3* RNAi was lower compared to *ani-1* RNAi, suggesting that multiple pathways also work in concert to control anterior epidermal cell migration. The netrin or ephrin pathways have been shown to function alongside the Slit/Robo pathway during ventral enclosure, and may therefore continue to work in concert during anterior morphogenesis (Bernadskaya et al., 2012). Further work depleting the Slit/Robo pathway components in specific tissues as well as temporally controlling the pathway so that it is only disrupted during anterior morphogenesis

would shed further light on the requirement for this pathway. The auxin-inducible-degron system is a tool that allows proteins to be degraded under the control of a tissue-specific promoter upon the addition of the plant hormone auxin (Zhang et al., 2015). Using this system with neuronal vs. epidermal specific promoters and exposing embryos to auxin during mid-embryogenesis would allow us to test the requirement for the Slit/Robo pathway as well as other pathways and components in neuronal versus epidermal tissues.

Morphogenetic events are required for the development and coordination of all metazoan tissues, and errors in these events can result in various diseases and birth defects. Despite these processes being so fundamental to development, very little is known about how different cell types communicate and coordinate themselves due to the intricacies of processes occurring at the cellular, tissue and multi-tissue level. We appreciate that there is a hierarchy of events that drive anterior morphogenesis that very few studies delve into when describing a developmental process for a complex structure that requires the coordination of multiple tissues. The initial characterization of the cell patterns, movements, and types during anterior morphogenesis set the foundation for not only better understanding this stage in *C. elegans* development but also for studying multi-tissue coordination as a whole. Uncovering the pathways that govern epidermal cell migration during anterior morphogenesis will not only provide new knowledge of how this process is regulated, but due to the conservation of these pathways among metazoans, can also provide insight as to how the development of more complex processes requiring multiple tissues occurs in other model systems.

CHAPTER 5
References

Ackley, B. D. (2014). Wnt-signaling and planar cell polarity genes regulate axon guidance along the anteroposterior axis in *C. elegans*. *Developmental Neurobiology*, *74*(8), 781–796. https://doi.org/10.1002/dneu.22146

Ahnn, J., & Fire, A. (1994). A screen for genetic loci required for body-wall muscle development during embryogenesis in *Caenorhabditis elegans*. *Genetics*, *137*(2), 483–498. https://doi.org/10.1093/genetics/137.2.483

Barnes, K. M., Fan, L., Moyle, M. W., Brittin, C. A., Xu, Y., Colón-Ramos, D. A., Santella, A., & Bao, Z. (2020). Cadherin preserves cohesion across involuting tissues during *C. Elegans* neurulation. *ELife*, *9*, 1–19. https://doi.org/10.7554/eLife.58626

Beatty, A., Morton, D., & Kemphues, K. (2010). The *C. elegans* homolog of Drosophila Lethal giant larvae functions redundantly with PAR-2 to maintain polarity in the early embryo. *Development (Cambridge, England)*, *137*(23), 3995–4004. https://doi.org/10.1242/DEV.056028

Bernadskaya, Y. Y., Wallace, A., Nguyen, J., Mohler, W. A., & Soto, M. C. (2012). UNC-40/DCC, SAX-3/Robo, and VAB-1/Eph Polarize F-Actin during Embryonic Morphogenesis by Regulating the WAVE/SCAR Actin Nucleation Complex. *PLoS Genetics*, *8*(8). https://doi.org/10.1371/journal.pgen.1002863

Bilder, D., Schober, M., & Perrimon, N. (2003). Integrated activity of PDZ protein complexes regulates epithelial polarity. *Nature Cell Biology 5*. https://doi.org/10.1038/ncb897

Blankenship, J. T., Backovic, S. T., Sanny, J. S. S. P., Weitz, O., & Zallen, J. A. (2006). Multicellular Rosette Formation Links Planar Cell Polarity to Tissue Morphogenesis.

Developmental Cell, *11*(4), 459–470. https://doi.org/10.1016/j.devcel.2006.09.007

Brenner, S. (1974). The genetics of *Caenorhabditis elegans*. *Genetics*, *77*(1), 71–94. https://doi.org/10.1093/genetics/77.1.71

Brose, K., Bland, K., Wang, K., Arnott, D., Henzel, W., Goodman, C., Tessier-Lavigne, M., & Kidd, T. (1999). Slit proteins bind Robo receptors and have an evolutionarily conserved role in repulsive axon guidance. *Cell*, *96*(6), 795–806. https://doi.org/10.1016/S0092-8674(00)80590-5

Chanal, P., & Labouesse, M. (1997). A screen for genetic loci required for hypodermal cell and glial-like cell development during Caenorhabditis elegans embryogenesis. *Genetics*, *146*(1), 207–226. /pmc/articles/PMC1207936/?report=abstract

Chin-Sang, I. D., George, S. E., Ding, M., Moseley, S. L., Lynch, A. S., & Chisholm, A. D. (1999). The ephrin VAB-2/EFN-1 functions in neuronal signaling to regulate epidermal morphogenesis in *C. elegans*. *Cell*, *99*(7), 781–790. https://doi.org/10.1016/S0092-8674(00)81675-X

Chisholm, A. D., & Hardin, J. (2005). Epidermal morphogenesis. *WormBook : The Online Review of C. Elegans Biology*, 1–22. https://doi.org/10.1895/wormbook.1.35.1

Clainche, C. Le, & Carlier, M.-F. (2008). Regulation of Actin Assembly Associated With Protrusion and Adhesion in Cell Migration. *Physiological Reviews*, *88*(2), 489–513. https://doi.org/10.1152/PHYSREV.00021.2007

Costa, M., Raich, W., Agbunag, C., B, L., Hardin, J., & Priess, J. R. (1998). A putative catenin-cadherin system mediates morphogenesis of the *Caenorhabditis elegans* embryo. *The Journal of Cell Biology*, *141*(1), 297–308. https://doi.org/10.1083/JCB.141.1.297

Drubin, D. G., & Nelson, W. J. (1996). Origins of Cell Polarity Review. In *Cell* (Vol. 84).

Fan, L., Kovacevic, I., Heiman, M. G., & Bao, Z. (2019). A multicellular rosette-mediated collective dendrite extension. *ELife*, *8*. https://doi.org/10.7554/eLife.38065

Fotopoulos, N., Wernike, D., Chen, Y., Makil, N., Marte, A., & Piekny, A. (2013). *Caenorhabditis elegans* anillin (ani-1) regulates neuroblast cytokinesis and epidermal morphogenesis during embryonic development. *Developmental Biology*, *383*(1), 61–74. https://doi.org/10.1016/j.ydbio.2013.08.024

Gettner, S. N., Kenyon, C., & Reichardt, L. F. (1995). Characterization of βpat-3 heterodimers, a family of essential integrin receptors in *C. elegans*. *Journal of Cell Biology*, *129*(4), 1127–1141. https://doi.org/10.1083/jcb.129.4.1127

Ghenea, S., Boudreau, J. R., Lague, N. P., & Chin-Sang, I. D. (2005). The VAB-1 Eph receptor tyrosine kinase and SAX-3/Robo neuronal receptors function together during *C. elegans* embryonic morphogenesis. *Development*, *132*(16), 3679–3690. https://doi.org/10.1242/dev.01947

Goley, E. D., & Welch, M. D. (2006). The ARP2/3 complex: An actin nucleator comes of age. In *Nature Reviews Molecular Cell Biology* (Vol. 7, Issue 10, pp. 713–726). https://doi.org/10.1038/nrm2026

Grimbert, S., Mastronardi, K., Richard, V., Christensen, R., Law, C., Zardoui, K., Fay, D., & Piekny, A. (2021). Multi-tissue patterning drives anterior morphogenesis of the *C. elegans* embryo. *Developmental Biology*, *471*, 49–64. https://doi.org/10.1016/j.ydbio.2020.12.003

Harding, M. J., McGraw, H. F., & Nechiporuk, A. (2014). The roles and regulation of multicellular rosette structures during morphogenesis. *Development (Cambridge)*, *141*(13), 2549–2558. https://doi.org/10.1242/dev.101444

Hoege, C., & Hyman, A. A. (2013). Principles of PAR polarity in *Caenorhabditis elegans*

embryos. In *Nature Reviews Molecular Cell Biology* (Vol. 14, Issue 5, pp. 315–322). https://doi.org/10.1038/nrm3558

Ikegami, R., Simokat, K., Zheng, H., Brown, L., Garriga, G., Hardin, J., & Culotti, J. (2012). Semaphorin and Eph receptor signaling guide a series of cell movements for ventral enclosure in *C. elegans*. *Current Biology*, *22*(1), 1–11. https://doi.org/10.1016/j.cub.2011.12.009

Kamath, R. S., Martinez-Campos, M., Zipperlen, P., Fraser, A. G., & Ahringer, J. (2001). Effectiveness of specific RNA-mediated interference through ingested double-stranded RNA in *Caenorhabditis elegans*. *Genome Biology*, *2*(1). https://doi.org/10.1186/gb-2000-2-1-research0002

Korswagen, H. C. (2002). Canonical and non-canonical Wnt signaling pathways in *Caenorhabditis elegans:* variations on a common signaling theme. *BioEssays*, *24*(9), 801–810. https://doi.org/10.1002/BIES.10145

Kuzmanov, A., Yochem, J., & Fay, D. S. (2014). Analysis of PHA-1 reveals a limited role in pharyngeal development and novel functions in other tissues. *Genetics*, *198*(1), 259–268. https://doi.org/10.1534/genetics.114.166876

Labouesse, M. (2006). Epithelial junctions and attachments. *WormBook : The Online Review of C. Elegans Biology*, 1–21. https://doi.org/10.1895/wormbook.1.56.1

Lecroisey, C., Ségalat, L., & Gieseler, K. (2007). The C. elegans dense body: Anchoring and signaling structure of the muscle. In *Journal of Muscle Research and Cell Motility* (Vol. 28, Issue 1, pp. 79–87). Springer Netherlands. https://doi.org/10.1007/s10974-007-9104-y

Low, I. I. C., Williams, C. R., Chong, M. K., McLachlan, I. G., Wierbowski, B. M., Kolotuev, I., & Heiman, M. G. (2019). Morphogenesis of neurons and glia within an epithelium.

Development (Cambridge), *146*(4). https://doi.org/10.1242/dev.171124

Mango, S. E. (2007). The *C. elegans* pharynx: a model for organogenesis. *WormBook : The Online Review of C. Elegans Biology*, 1–26. https://doi.org/10.1895/wormbook.1.129.1

Mango, S. E., Lambie, E. J., & Kimble, J. (1994). The pha-4 gene is required to generate the pharyngeal primordium of *Caenorhabditis elegans*. *Development*, *120*(10), 3019–3031. https://doi.org/10.1242/dev.120.10.3019

Martin, A. C., & Goldstein, B. (2014). Apical constriction: Themes and variations on a cellular mechanism driving morphogenesis. In *Development (Cambridge)* (Vol. 141, Issue 10, pp. 1987–1998). Company of Biologists Ltd. https://doi.org/10.1242/dev.102228

Mentink, R. A., Middelkoop, T. C., Rella, L., Ji, N., Tang, C. Y., Betist, M. C., vanOudenaarden, A., & Korswagen, H. C. (2014). Cell intrinsic modulation of wnt signaling controls neuroblast migration in c.elegans. *Developmental Cell*, *31*(2), 188–201. https://doi.org/10.1016/j.devcel.2014.08.008

Motegi, F., & Sugimoto, A. (2006). Sequential functioning of the ECT-2 RhoGEF, RHO-1 and CDC-42 establishes cell polarity in *Caenorhabditis elegans* embryos. *Nature Cell Biology 2006 8:9*, *8*(9), 978–985. https://doi.org/10.1038/ncb1459

Munro, E., Nance, J., & Priess, J. R. (2004). Cortical Flows Powered by Asymmetrical Contraction Transport PAR Proteins to Establish and Maintain Anterior-Posterior Polarity in the Early *C. elegans* Embryo. *Developmental Cell*, *7*(3), 413–424. https://doi.org/10.1016/J.DEVCEL.2004.08.001

Nobes, C. D., & Hall, A. (1995). Rho, Rac, and Cdc42 GTPases regulate the assembly of multimolecular focal complexes associated with actin stress fibers, lamellipodia, and filopodia. *Cell*, *81*(1), 53–62. https://doi.org/10.1016/0092-8674(95)90370-4

Ouellette, M. H., Martin, E., Lacoste-Caron, G., Hamiche, K., & Jenna, S. (2016). Spatial control of active CDC-42 during collective migration of hypodermal cells in *Caenorhabditis elegans*. *Journal of Molecular Cell Biology*, *8*(4), 313–327. https://doi.org/10.1093/jmcb/mjv062

Patel, F. B., Bernadskaya, Y. Y., Chen, E., Jobanputra, A., Pooladi, Z., Freeman, K. L., Gally, C., Mohler, W. A., & Soto, M. C. (2008). The WAVE/SCAR complex promotes polarized cell movements and actin enrichment in epithelia during *C. elegans* embryogenesis. *Developmental Biology*, *324*(2), 297–309. https://doi.org/10.1016/j.ydbio.2008.09.023

Portereiko, M. F., & Mango, S. E. (2001). Early morphogenesis of the *Caenorhabditis elegans* pharynx. *Developmental Biology*, *233*(2), 482–494. https://doi.org/10.1006/dbio.2001.0235

Portereiko, M. F., Saam, J., & Mango, S. E. (2004). ZEN-4/MKLP1 is required to polarize the foregut epithelium. *Current Biology*, *14*(11), 932–941. https://doi.org/10.1016/j.cub.2004.05.052

Raich, W. B., Agbunag, C., & Hardin, J. (1999). Rapid epithelial-sheet sealing in the *Caenorhabditis elegans* embryo requires cadherin-dependent filopodial priming. *Current Biology*, *9*(20), 1139–1146. https://doi.org/10.1016/S0960-9822(00)80015-9

Rapti, G., Li, C., Shan, A., Lu, Y., & Shaham, S. (2017). Glia initiate brain assembly through noncanonical Chimaerin-Furin axon guidance in *C. elegans*. *Nature Neuroscience*, *20*(10), 1350–1360. https://doi.org/10.1038/nn.4630

Rasmussen, J. P., Reddy, S. S., & Priess, J. R. (2012). Laminin is required to orient epithelial polarity in the *C. elegans* pharynx. *Development*, *139*(11), 2050–2060. https://doi.org/10.1242/dev.078360

Ridley, A. J., Schwartz, M. A., Burridge, K., Firtel, R. A., Ginsberg, M. H., Borisy, G., Parsons,

J. T., & Horwitz, A. R. (2003). Cell Migration: Integrating Signals from Front to Back. In *Science* (Vol. 302, Issue 5651, pp. 1704–1709). American Association for the Advancement of Science. https://doi.org/10.1126/science.1092053

Rodriguez-Boulan, E., & Macara, I. G. (2014). Organization and execution of the epithelial polarity programme. *Nature Reviews Molecular Cell Biology 2014 15:4*, *15*(4), 225–242. https://doi.org/10.1038/nrm3775

Rodriguez-Diaz, A., Toyama, Y., Abravanel, D. L., Wiemann, J. M., Wells, A. R., Tulu, U. S., Edwards, G. S., & Kiehart, D. P. (2008). Actomyosin purse strings: renewable resources that make morphogenesis robust and resilient. *HFSP Journal*, *2*(4), 220. https://doi.org/10.2976/1.2955565

Rørth, P. (2009). Collective cell migration. *Annual Review of Cell and Developmental Biology*, *25*, 407–429. https://doi.org/10.1146/annurev.cellbio.042308.113231

Shah, P. K., Tanner, M. R., Kovacevic, I., Rankin, A., Marshall, T. E., Noblett, N., Tran, N. N., Roenspies, T., Hung, J., Chen, Z., Slatculescu, C., Perkins, T. J., Bao, Z., & Colavita, A. (2017). PCP and SAX-3/Robo Pathways Cooperate to Regulate Convergent Extension-Based Nerve Cord Assembly in *C. elegans. Developmental Cell*, *41*(2), 195-203.e3. https://doi.org/10.1016/j.devcel.2017.03.024

Sharma, M., Castro-Piedras, I., Simmons, G. E., Jr, & Pruitt, K. (2018). Dishevelled: a masterful conductor of complex Wnt signals. *Cellular Signalling*, *47*, 52. https://doi.org/10.1016/J.CELLSIG.2018.03.004

Skiba, F., & Schierenberg, E. (1992). Cell lineages, developmental timing, and spatial pattern formation in embryos of free-living soil nematodes. *Developmental Biology*, *151*(2), 597–610. https://doi.org/10.1016/0012-1606(92)90197-O

Song, S., Zhang, B., Sun, H., Li, X., Xiang, Y., Liu, Z., Huang, X., & Ding, M. (2010). A wnt-frz/ror-dsh pathway regulates neurite outgrowth in *caenorhabditis elegans*. *PLoS Genetics*, *6*(8), 1001056. https://doi.org/10.1371/journal.pgen.1001056

Sternberg, P. W. (1988). Lateral inhibition during vulval induction in *Caenorhabditis elegans. Nature*, *335*(6190), 551–554. https://doi.org/10.1038/335551a0

Sternberg, P. W. (2005). Vulval development. In *WormBook : the online review of C. elegans biology* (pp. 1–28). WormBook. https://doi.org/10.1895/wormbook.1.6.1

Sternberg, P. W., & Horvitz, H. R. (1986). Pattern formation during vulval development in *C. elegans*. *Cell*, *44*(5), 761–772. https://doi.org/10.1016/0092-8674(86)90842-1

Sulston, J. E., Schierenberg, E., White, J. G., & Thomson, J. N. (1983). The embryonic cell lineage of the nematode *Caenorhabditis elegans*. In *Developmental Biology* (Vol. 100, Issue 1, pp. 64–119). https://doi.org/10.1016/0012-1606(83)90201-4

Vitorino, P., & Meyer, T. (2008). Modular control of endothelial sheet migration. *Genes & Development*, *22*(23), 3268–3281. https://doi.org/10.1101/GAD.1725808

Watts, J. L., Etemad-Moghadam, B., Guo, S., Boyd, L., Draper, B. W., Mello, C. C., Priess, J. R., & Kemphues, K. J. (1996). par-6, a gene involved in the establishment of asymmetry in early *C. elegans* embryos, mediates the asymmetric localization of PAR-3. *Development*, *122*(10), 3133–3140. https://doi.org/10.1242/dev.122.10.3133

Wernike, D., Chen, Y., Mastronardi, K., Makil, N., & Piekny, A. (2016). Mechanical forces drive neuroblast morphogenesis and are required for epidermal closure. *Developmental Biology*, *412*(2), 261–277. https://doi.org/10.1016/j.ydbio.2016.02.023

White, J. G., Southgate, E., Thomson, J. N., & Brenner, S. (1986). The structure of the nervous system of the nematode *Caenorhabditis elegans*. *Philosophical Transactions of the Royal*

Society of London. B, Biological Sciences, *314*(1165), 1–340. https://doi.org/10.1098/rstb.1986.0056

Williams-Masson, E. M., Heid, P. J., Lavin, C. A., & Hardin, J. (1998). The cellular mechanism of epithelial rearrangement during morphogenesis of the *Caenorhabditis elegans* dorsal hypodermis. *Developmental Biology*, *204*(1), 263–276. https://doi.org/10.1006/dbio.1998.9048

Williams-Masson, E. M., Malik, A. N., & Hardin, J. (1997). An actin-mediated two-step mechanism is required for ventral enclosure of the *C. elegans* hypodermis. *Development*, *124*(15), 2889–2901. https://doi.org/10.1242/dev.124.15.2889

Williams, B. D., & Waterston, R. H. (1994). Genes critical for muscle development and function in *Caenorhabditis elegans* identified through lethal mutations. *Journal of Cell Biology*, *124*(4), 475–490. https://doi.org/10.1083/jcb.124.4.475

Zallen, J. A., Kirch, S. A., & Bargmann, C. I. (1999). Genes required for axon pathfinding and extension in the *C. elegans* nerve ring. *Development*, *126*(16), 3679–3692. https://doi.org/10.1242/DEV.126.16.3679

Zallen, J. A., Yi, B. A., & Bargmann, C. I. (1998). The Conserved Immunoglobulin Superfamily Member SAX-3/Robo Directs Multiple Aspects of Axon Guidance in *C. elegans*. *Cell*, *92*(2), 217–227. https://doi.org/10.1016/S0092-8674(00)80916-2

Zecca, M., Basler, K., & Struhl, G. (1996). Direct and long-range action of a wingless morphogen gradient. *Cell*, *87*(5), 833–844. https://doi.org/10.1016/S0092-8674(00)81991-1

Zhang, L., Ward, J. D., Cheng, Z., & Dernburg, A. F. (2015). The auxin-inducible degradation (AID) system enables versatile conditional protein depletion in *C. elegans*. *Development*, *142*(24), 4374–4384. https://doi.org/10.1242/DEV.129635